

รายงานวิจัยฉบับสมบูรณ์

โครงการ การศึกษาโครงสร้างและหน้าที่ของโปรตีนสารพิษฆ่าลูกน้ำยุง จากแบคทีเรีย Bacillus sphaericus

Structure-Function Studies of The Bacillus sphaericus Binary Toxin

โดย นางสาวปนัดดา บุญเสริม

สิงหาคม 2550

Acknowledgements

This work was supported the Thailand Research Fund, the National Center for Genetic Engineering and Biotechnology, National Science and Technology Development Agency, Thailand, the Commission on Higher Education, Thailand, and the Biomedical Research Council, Singapore. We are also grateful to Ms. Somsri Sakdee and Ms. Chaweewan Shimwai for technical assistance.

บทคัดย่อ

รหัสโครงการ RSA4780008

ชื่อโครงการ การศึกษาโครงสร้างและหน้าที่ของโปรตีนสารพิษฆ่าลูกน้ำยุงจากแบคทีเรีย Bacillus sphaericus

ชื่อหักวิจัย ผู้ช่วยศาสตราจารย์ปนัดดา บุญเสริม

E-mail Address: mbpbs@mahidol.ac.th

ระยะเวลาโครงการ 3 ปี

แบคทีเรีย Bacillus sphaericus สามารถสร้างโปรตีน binary toxin ซึ่งประกอบด้วยโปรตีน BinA และ BinB ที่มี ฤทธิ์ฆ่าลูกน้ำยุง โปรตีน BinB ทำหน้าที่จับกับตัวตอบรับ ในขณะที่ BinA ทำหน้าที่ในการออกฤทธิ์ฆ่าลูกน้ำยุงโดยยังไม่ ทราบกลไกที่แน่ชัด โครงการวิจัยนี้ได้ทำการศึกษาโครงสร้างระดับทุติยภูมิของโปรตีน BinA และ BinB ในสภาวะที่มี และ ไม่มีไขมัน โดยการใช้เทคนิค Fourier transform infrared spectroscopy (attenuated total reflection, ATR-FTIR) ผลการ ทดลองพบว่าโปรตีนทั้งสองชนิดมีการเปลี่ยนแปลงโครงสร้างระดับทุติยภูมิเมื่ออยู่ในสภาวะที่มีชั้นไขมัน (lipid bilayers) และการเปลี่ยนแปลงโครงสร้างดังกล่าวนี้จะแตกต่างกันระหว่างโปรตีนทั้งคู่อยู่แยกกัน และโปรตีนทั้งคู่อยู่รวมกันแสดงว่า การม้วนพับของโปรตีนให้ได้โครงสร้างที่เหมาะสมนั้นอาศัยโปรตีนทั้งสองชนิด นอกจากนี้ยังพบว่าโปรตีน BinB เท่านั้นที่ สามารถสอดแทรกเข้าสู่ชั้นไขมัน (lipid monolayers) ได้ และเพื่อเพิ่มความเข้าใจในกลไกการทำงานของโปรตีน binary toxin งานวิจัยนี้ยังได้ศึกษาความสำคัญของกรดอะมิโน Cysteine ที่อนุรักษ์ใน BinA (C31 C47 และ C195) และ BinB (C67 C161 และ C241) โดยการเปลี่ยนแปลงกรดอะมิโนดังกล่าว โดยพบว่าโปรตีนกลายพันธุ์ส่วนใหญ่มีความสามารถใน การฆ่าลูกน้ำยุงลดลงมาก ยกเว้นโปรตีนกลายพันธุ์จากการเปลี่ยนกรดอะมิโน C241 ใน BinB ซึ่งยังคงมีความสามารถใน การออกฤทธิ์อยู่ และการสูญเสียความสามารถในการฆ่าลูกน้ำยุงนี้ไม่เกี่ยวข้องกับการสร้างพันธะ disulphide ภายใน โมเลกุลของ BinA และ BinB อย่างไรก็ตามกรดอะมิโน cysteine เหล่านี้อาจมีความสำคัญต่อการรวมกลุ่มของโมเลกุล โปรตีน (oligomerisation) การจับกันระหว่างโปรตีน BinA และ BinB หรือการจับกับตัวตอบรับ นอกจากนี้ยังได้ ทำการศึกษาบทบาทของกรดอะมิโนที่มีประจุบางตัวในโปรตีน BinA (R97 E98 R101 และ E114) โดยการแทนที่ด้วย กรดอะมิโน Alanine พบว่าโปรตีนกลายพันธุ์ทั้งหมดมีความสามารถในการฆ่าลูกน้ำยุงลดลงอย่างมาก แสดงว่ากรดอะมิโน เหล่านี้มีความสำคัญต่อการออกฤทธิ์ฆ่าลูกน้ำยุง และความสามารถในการฆ่าลูกน้ำยุงที่ลดลงของโปรตีนกลายพันธุ์เหล่านี้ ไม่สัมพันธ์กับความสามารถในการจับกันระหว่างโปรตีน BinA และ BinB ดังนั้นจึงจำเป็นต้องทำการศึกษาบทบาทของ กรดอะมิโนที่มีประจุเหล่านี้ต่อกลไกที่เกี่ยวข้องกับการออกฤทธิ์ฆ่าลูกน้ำยุงต่อไปในอนาคต

Abstract

Project Code: RSA4780008

Project Title: Structure-Function Studies of the Bacillus sphaericus Binary Toxin

Investigator: Assistant Professor Panadda Boonserm

Institute of Molecular Biology and Genetics, Mahidol University

E-mail Address: mbpbs@mahidol.ac.th

Project Period: 3 years

Bacillus sphaericus (Bs) produces mosquito-larvicidal binary toxin (BinA and BinB) during its sporulation. BinB has been identified as receptor-binding subunit while BinA is expected to bind to BinB and exert its activity via unknown mechanism. Structural characterisation of the binary toxin components was performed using Fourier transform infrared spectroscopy (attenuated total reflection method, ATR-FTIR) to demonstrate the secondary structures of the binary toxin in the absence and in the presence of lipids. Upon interaction with lipid bilayers, a dramatic conformational change involving secondary structure changes was observed in both BinA and BinB. Upon membrane association, the change in conformation observed for BinA or BinB separately is different from that observed when the proteins are combined, indicating that proper folding depends on the presence of the complementary subunit. It is also demonstrated in this study that BinB, but not BinA, is able to insert in model neutral lipid monolayers. To better understand the mechanism of the binary toxin, amino acid substitutions of three conserved cysteine residues in BinA (C31, C47, and C195) and BinB (C67, C161, and C241) were performed. Substitutions of most cysteine residues in both BinA and BinB were found to dramatically reduce or abolish their toxicity except mutation of C241-BinB which still retained its larvicidal activity. The loss of toxicity was not due to the disulphide bond formation within BinA and BinB molecules, however, these cysteine residues may play a critical role during oligomerisation, interaction between BinA and BinB or receptor binding. addition, some selected charged residues of BinA (R97, E98, R101, and E114) were substituted with alanine to study their roles in biological activity. All mutants were found to drastically reduce the toxicity indicating that these four charged residues are essential for the full toxicity of the binary toxin. Binding ability between BinA and BinB was not correlated with the reduced toxicity of these mutants. Therefore, the roles of these charged residues on the other steps involved in the full toxicity are required to be investigated further.

1. Introduction

Many strains of *Bacillus sphaericus* (Bs) produce a binary toxin which is highly active against the larvae of *Culex* and *Anopheles* mosquitoes. The same toxin, however, is only mildly toxic or non toxic to *Aedes* [1]. This toxin is composed of two proteins, 42 kDa (BinA) and 51 kDa (BinB), which are deposited as parasporal crystals during sporulation [2]. Both proteins are required for larvicidal activity, and maximal toxicity is observed when they are present in equimolar amounts [3;4], although at high concentrations, even BinA alone can be toxic to cultured *Culex* cells [5-8].

After the crystal toxins are ingested by the susceptible larvae, crystalline inclusions are solubilized in the alkaline pH of the larvae midgut, followed by activation by larval proteases, and binding of toxin proteins to the gastric cecum and posterior midgut [9]. It has been demonstrated that BinB is the primary binding component, and directs the localized binding of BinA [10]. Subsequent internalisation of the binary toxin following binding has been observed, and it has been suggested to be correlated with toxicity [11]. In *Culex pipiens* larvae, the putative receptor has been identified as α -glucosidase [12] and this receptor has been cloned [13]. However, the detailed mechanism that leads to the death of mosquito larvae, after binding of the toxin complex, is not clearly understood.

Ultrastructural observations [14-16] have shown profound morphological changes of the larval midgut epithelial cells. Also, electrophysiological studies conducted on cultured *Culex quinquefasciatus* cells have provided evidence that the activated binary toxin, like *Bacillus thuringiensis* (Bt) toxins, interacts with cell membranes and may form pores [17]. Support for binary toxin-induced membrane permeabilisation has been provided by a study of channel activity and membrane permeability using a receptor-free planar lipid bilayer and large unilamellar phospholipid vesicles. In this study, BinA, and to a lesser extent BinB, were suggested to increase permeability [18].

Despite these initial studies, structural information on this system, both in terms of secondary and tertiary structure, is lacking. Crucially, the structural changes that may take place simultaneously with membrane association and dimer formation and possibly oligomerization have not been studied. Infrared spectroscopy is specially suitable for the study of membrane proteins [19;20] and, especially, to monitor structural changes that take place in facultative

membrane proteins during the transition from aqueous solution to the membrane environment. Therefore, to provide further insight into the interaction of the binary toxin components with lipid membranes, we have investigated their secondary structure in the absence and in the presence of lipids, using attenuated total reflection Fourier transform infrared spectroscopy (ATR-FTIR). We have also monitored the membrane insertion of each of these components in a model lipid monolayer. Our results clearly demonstrate that the interaction of the binary toxin components with the lipid membrane is accompanied by a dramatic conformational change.

To gain further understanding of the mode of toxic action of the binary toxin, amino acid substitutions of the selected residues in BinA and BinB were performed. Effects of amino acid substitutions on expression level, inclusion formation, overall tertiary structure, formation of the BinA and BinB complex and toxicity to mosquito larvae were investigated.

2. Materials and Methods

- **2.1 Construction of mutant plasmids** Site-directed mutagenesis technique was exploited to generate mutant plasmids. The pGEX-BinA plasmid expressing GST-BinA fusion protein, pET17b plasmid expressing the truncated BinB under control of T7 promoter, were used as the templates for PCR-based site-directed mutagenesis by using complementary oligonucleotide primers containing the required mutation. The restriction endonuclease digestion was used to screen the desired mutant plasmids based on their recognition sites incorporated mutagenic primers. The DNA sequence of the obtained plasmid was confirmed by automated DNA sequencing analysis.
- 2.2 Protein preparation. Escherichia coli BL21 (DE3) pLysS clones harbouring the recombinant plasmids [21] were grown at 37°C in a Luria–Bertani medium containing 100 μg/ml ampicillin and 34 µg/ml chloramphenecol until OD600 of the culture reached 0.3–0.5. Protein expression was induced with isopropyl-β-D-thiogalactopyranoside (IPTG) at a final concentration of 0.1 mM. The culture was further incubated at 37°C for 5 h. E.coli cultures overexpressing the binary toxin as cytoplasmic inclusions were harvested by centrifugation and suspended cells were then disrupted by 3 times of French Press at 10,000 psi. Protein concentrations of the partial-purified inclusions were determined by using a protein microassay reagent (Bio-Rad), with a bovine serum albumin fraction V (Sigma) as a standard. Inclusions (1-2 mg/ml) were solubilised by incubation at 37°C for 1 h in 25mM NaOH, 5 mM DTT. Solubilised protoxins were then separated from insoluble materials by centrifugation at 12000g for 15 min. Soluble protein was stepwise dialysed in carbonate buffer (50 mM Na₂CO₃, pH 10.0), and concentrated by ultrafiltration at 4°C using a Centriprep column (30-kDa cutoff, Amicon). The protein was further purified by a size-exclusion FPLC system (Superose 12 HR 10/30, Amersham-Pharmacia Biotech) with a linear gradient of 50mM Na₂CO₃, pH 10.0, 1 mM DTT at a flow rate of 0.4ml/min.
- **2.3 Protocol for ATR-FTIR.** Infrared spectra were recorded on a Nicolet Nexus spectrometer (Madison, USA) purged with N_2 and equipped with a MCT/A detector, cooled with liquid nitrogen. Attenuated total reflection (ATR) spectra were measured with a 25-reflections ATR accessory from Graseby Specac (Kent, UK) and a wire grid polarizer (0.25 μ m, Graseby Specac). A total of 200 interferograms collected at a resolution of 4 cm⁻¹ were averaged for every sample and processed with 1 point zero filling and Happ-Genzel apodization.

- 2.4 Incorporation of the protein to DMPC bilayers. Sample preparation was performed essentially as described previously [22]. Initially, DMPC was solubilized in ethanol, and dried after exposure to air. The purified protein was added to the dry lipid in 50 mM sodium carbonate buffer, pH 10, at a concentration of 1 mg/ml. The total lipid (DMPC):protein molar ratio was 100:1. Approximately 100 μ l of this solution, containing protein in the presence of multilamelar liposomes, was deposited in successive aliquots of 10 μ l onto a trapezoidal (50mm \times 2mm \times 20mm) Ge internal reflection element (IRE). Bulk water was removed using a dry N_2 stream through the ATR compartment to form regular stacks of lipid bilayers parallel to the internal reflection element surface. For transmission experiments, the protein dissolved in buffer was previously lyophilized and later solubilized with 100 μ l of D_2O . This solution was transferred to a rectangular transmission cell with CaF_2 windows.
- **2.5 Infrared data analysis.** The secondary structure composition of (i) BinA, (ii) BinB and (iii) the mixture BinA/BinB at 1:1 molar ratio, was obtained by analysing the amide I band, and using previous assignments [23]. Main bands were identified after mild Fourier deconvolution (FWHH 20 cm^{-1} and k 1.5) and curvefitted to obtain component bands after subtracting the contribution of amino acid side chain absorption to the amide I [24]. The spectrum in the amide I region corresponding to the side chains was subtracted from the experimental amide I until the band corresponding to protonated tyrosine, at 1515 cm^{-1} , was eliminated. Dichroic ratios were calculated as the ratio between the integrated absorptions of the spectra collected with parallel and perpendicular polarized light. Isotopic exchange (Hydrogen /Deuterium, H/D) was calculated from the ratio Amide II / Amide I before and after exchange, using the non polarised spectra. Non polarized spectra were obtained from the parallel (||) and perpendicularly (\perp) ATR polarized spectra, using the expression 1 (||) + 1.44 (\perp) as described previously [25].
- **2.6 Preparation of LB Monolayers.** The interaction of BinA and BinB with DMPC lipid monolayers was monitored using a constant surface pressure assay [26] using a NIMA Langmuir-Blodgett (LB) trough 611 (Coventry, UK). Before starting the experiment, the trough was cleaned successively with chloroform or ethanol, followed by rinsing with deionized water. Carbonate buffer pH 10.0 was used as the subphase. DMPC dissolved in chloroform was spread on the surface of the buffer. After 15-20 min, the monolayer was compressed at a speed of 10 cm²/min, until the surface pressure reached 25 mN/m. Control injections containing only buffer were delivered into the subphase before each experiment. The sample containing the protein was

then injected (3-5 nmoles) through an L-shaped syringe from underneath the Teflon barrier. All experiments were performed at room temperature.

- **2.7 Dynamic light scattering measurements.** Dynamic Light Scattering (DLS) measurements were performed using a 90 Plus particle size analyzer (Brookhaven Instruments Corp).
- **2.8 Intrinsic fluorescent property analysis.** Fluorescence spectra of the wild type BinA and its mutants were obtained by emission scanning of protein solution in a 10 mm path length square quartz cell. The protein samples were excited at 280 nm using a Jasco FP-6500 spectrofluorometer. The Emission spectra were recorded from 300-500 nm with medium scanning speed using 3 nm of excitation and emission slit width. All spectra were subtracted with baseline spectra from buffer.
- 2.9 Dot blot analysis. 2.5-40 μg of purified BinB was loaded on membrane. The membrane containing immobilized BinB was blocked with 5% skim milk for 3 hours at 4°C. The membrane was then overlaid with 100 μg/ml of purified GST-BinA or its mutants in 5% skim milk in 1X PBS buffer for 1 hour and subsequently washed with 0.1% Tween20 in 1X PBS buffer for 3 times, 5 minutes each. The bound GST-BinA was detected by probing with mouse anti-GST antibody (1:2,500) and kept at room temperature with gently shaking for 1 hour. The unbound proteins were removed by washing with the same buffer for 3 times, 5 minutes each. The membranes were subsequently incubated with goat anti-mouse HRP conjugate (1:5,000) at room temperature with gently shaking for 1 hour and membrane was washed with 0.1% Tween20 in 1X PBS buffer for 2 times 5 minutes each following by washing with 1X PBS buffer for 5 minutes. The signal on the membrane was then detected by using the reaction mixtures consist of 0.012 g DAB, 0.008 g NiCl₂, 1 ml of 0.5 M Tris pH 7.4 and 16.8 ml of HPLC water. 200 μl of H₂O₂ was immediately added before detection.
- 2.10 Mosquito larvicidal assays. Mosquito larvicidal assays were performed in duplicate using 2^{nd} instar *C. quinquefasciatus* larvae supplied by the mosquito rearing facility from the Institute of Molecular Biology and Genetics, Mahidol University. Mosquito larvicidal activity was tested by mixing BinA and BinB inclusions at 1:1 molar ratio and diluted as 2-fold serial dilution. Six to eight concentrations were used for each toxin, and in case of very low toxic mutants, a single-dosed protein concentration at 50 µg/ml was used. One ml of diluted protein was added to 1 ml of water containing 10 larvae in each well of 24-well tissue culture plate (diameter of the well is

- 1.5 cm). Mortality was recorded after incubation at 30°C for 48 hours. LC50 was determined using Probit analysis.
- **2.11 Lipid vesicle preparation.** Multilarmillar liposomes were prepared by mixing 10 mg/ml of PC (phosphatidylcholine) and cholesterol with the ratio of 8:2 (v:v). Lipid solution was dried under Nitrogen gas and resuspended in 10 mM of Tris-HCl, pH 9 and 0.5 M Na₂CO₃ pH 9. The mixture was vortexed vigorously for 10 minutes before used.
- **2.12 Proteolysis of lipid-incorporated protein with proteinase K.** 5 mg/ml of multilarmillar liposomes was incubated with 2 mg/ml of truncated BinB in total volume 750 ul at room temperature for 2 hours. Then 0.2 mg/ml of proteinase K was added to the reaction and further incubated for 2 hours. The digested protein was removed by centrifugation at 13,000 rpm for 30 minutes. The supernatant was precipitated by acetone and kept for analysis on SDS-PAGE. Pellet containing liposome with incorporated protein was resuspended in acetone. The reaction mixture was further incubated for 30 minutes at room temperature before collecting the precipitated protein in the pellet by centrifugation at 13,000 rpm.

3. Results and Discussion

3.1 Amide proton exchange.

To determine the percentage of proton exchange resistant amide groups, we exposed the purified protein samples to D₂O (see Materials and Methods), and monitored the changes in intensity in the bands amide II and amide A. Fig. 1 shows that when BinA or BinB were reconstituted in the presence of liposomes, the amide II band (N-H bending) at ~1550 cm⁻¹ disappeared after D₂O equilibration (see arrows in Fig. 1B and D) suggesting complete exchange. However, inspection of the amide A, due to N-H stretching, (Fig. 1A, C, dotted line), showed a small band representing non-exchanged amide protons. The area of this remaining band corresponds to approximately 10 % of the total amide A before deuterium exchange (shown in Fig. 1A, C, solid line). This percentage corresponds to approximately 40 amino acids. A similar percentage for this residual amide A was obtained for BinA, BinB or the mixture BinA/BinB (not shown). The lack of complete exchange does not necessarily imply partial insertion in the membrane, and it could be originated by simple membrane association, or the presence of slow-exchanging secondary structures.

3.2. Investigation of the membrane insertion of each of binary toxin components in a model lipid monolayer

We investigated the membrane insertion of binary toxin components by using a Langmuir-Blodgett trough. Figure 2 shows that when BinA or BinB was injected in the subphase of the trough, only BinB inserted in the DMPC monolayer (Fig. 2A, solid line). When BinA and BinB were mixed and added to the subphase (Fig. 2B), insertion was also observed, and to the same extent as that observed for BinB alone, although with different kinetics. The fact that the extent of insertion was the same for BinB and the mixture BinA/BinB suggests that in both cases only BinB inserts. The kinetics are however affected by the presence of BinA, which probably induces conformational changes in BinB. The difference in behavior between BinA and BinB is consistent with their suggested separate roles *in vivo*, with only BinB being responsible for binding to a membrane receptor.

The membrane inserted residues in BinB, which only constitute a 10% of the total (see above), could be inserted as α -helices, forming a α -helical hairpin, similar to those described for Cry toxins [27]. Alternatively, oligomerization of the toxins could lead to formation of a

transmembrane β -barrel, which could also explain a pore behaviour. To examine these two possibilities, we used the fact that the amide A frequency is sensitive to secondary structure, and shifts towards higher frequencies for α -helical structures, reflecting the presence of weaker hydrogen bonds than those found in β -sheets [28]. Therefore, we examined the frequency of amide A in the mixture BinA/BinB in the presence of lipid bilayers, after D₂O equilibration (Fig. 3A). In these conditions, the amide A only corresponds to the part of the protein that is inserted in the membrane. We then compared the frequency of this band to that of peptides known to adopt either a completely α -helical or β structural conformation (see Fig. 3, legend). The secondary structure of these model peptides is either α -helical, with amide I centered at 1656 cm⁻¹ or β -structure, with amide I centered at 1628 cm⁻¹, respectively (shown in Fig. 3B). Fig. 3A shows that the amide A corresponding to the protected residues in the mixture BinA/BinB (Fig. 3A, solid line) is similar to that of the peptide that adopts a β structure (Fig. 3A, dotted line), suggesting that the protected residues in BinA/BinB are mostly in a β -sheet conformation. For BinA, which showed no insertion (Fig. 2), the amide A was broader, and centered between that of the α and β model peptides (not shown).

Overall, this suggests that the membrane inserted residues in BinB and BinA/BinB adopt a β -sheet conformation, not α -helical, suggesting that the putative pores formed by this binary toxin consist of β -barrels. Further, the dichroic ratio for the amide A was 1.9±0.1, which is compatible with typical β -barrel dichroic ratios [29].

3.3. Conformational change after membrane association

In proteins, the amide I region of the infrared spectrum is sensitive to the secondary structure content. Figure 4 shows the amide I region for BinA, BinB and their mixture, both in solution and in the presence of lipid bilayers. For BinA, in aqueous solution, i.e., in the absence of membranes, the amide I shows an intense band at 1673 cm⁻¹ (Fig. 4A, solid line) that we assign to β-turns (see Materials and methods). In contrast, when BinA was prepared in the presence of lipid bilayers in bulk H₂O (Fig. 4A, broken line), a more heterogeneous spectrum was observed, with features at 1685, 1660, and 1640 cm⁻¹ (see deconvoluted spectra in Fig. 4B), with most of the intensity in the latest band (1640 cm⁻¹), that we assign to β strands. When this sample was equilibrated in D₂O (Fig. 4A, dotted line), a small shift was observed in all the amide

I bands, consistent with amide proton exchange. A similar behavior was observed for BinB (Figs. 4C and D), although in solution (Fig. 4C, solid line), the spectrum appears more homogeneous than for BinA, with almost no features below 1660 cm⁻¹. These data clearly show, therefore, that interaction of either BinA or BinB with lipid bilayers results in a dramatic conformational change that involves not only changes in tertiary structure, but even variations in secondary structure that affect most of the molecule. Fig. 4E (solid line) shows that the mixture BinA/BinB, either in solution or in the absence of membranes, is not a sum of the spectra for BinA and BinB in the same conditions, therefore BinA and BinB interact when they are in aqueous solution, i.e., before their interaction with lipid bilayers. The spectrum of this mixture in solution shows a band at 1630 cm⁻¹ which we assign to β structure. No other features are observed in the amide I. Further, when the mixture BinA/BinA interacts with membranes (Fig. 4E, broken line and dotted line), the spectrum suffers a dramatic change. In the presence of membranes exposed to H₂O (Fig. 4E, broken line), the band at 1630 cm⁻¹ disappears and other bands are observed. One of these additional bands is centered at 1685 cm⁻¹ and, upon exposure to D₂O (Fig. 4E, dotted line), it shifts to 1676 cm⁻¹, which is similar to the band observed when BinA or BinB is in D₂O solution. This clearly shows that the end product of the folding elicited by contact of either BinA or BinB with the membrane is not the same as that observed for the mixture BinA/BinB. When the latter species binds to the membrane, the resulting structure contains elements of the individual proteins in solution and in a membrane-bound state.

3.4 Substitutions of the conserved cysteine residues in BinA and BinB proteins and their effects on the mosquito-larvicidal activity

Amino acid sequence analysis of BinA and BinB proteins from different strains of *B. sphaericus* revealed that all of them share very high homology with more than 90% amino acid identity [30;31]. It has been found that the active cores of BinA and BinB contain cysteine residues that are highly conserved among various strains of *B. sphaericus*. It is possible that some of these cysteine residues may play a key role in maintaining the tertiary structures or may be critical for intermolecular interaction between BinA and BinB proteins.

The role of cysteine on the biological activity of BinA was investigated by substituting each of three conserved cysteine residues at positions 31, 47, and 195 with either alanine or serine. Each of these mutants was found to be over-expressed as inclusion bodies similar to the

Substitution at Cys195 significantly reduced the toxin activity against *Culex* wild type. quinquefasciatus larvae whereas substitution at Cys31 and Cys47 abolished its toxicity (Table 1). All double and triple mutants were found to be inactive (Table 1). Intrinsic fluorescent analysis suggested that all mutant proteins should have similar tertiary structure to that of the wild type (data not shown). To investigate whether these residues are involved in disulfide bond formation, the wild type and mutant proteins were subjected to analyze on SDS-PAGE with and without reducing agent (10 mM DTT). Two different sample preparations were used in this analysis. The first sample preparation used partially purified inclusions and the second preparation used proteins that were solubilized in 25 mM NaOH and subsequently dialyzed in 50 mM Na₂CO₃ pH 10.5. Samples from both preparations were mixed with SDS-PAGE sample buffer with and without 10 mM DTT. Results in figure 5 demonstrated that the mobility of the major band corresponding to BinA protein was not different between samples with and without reducing agent in both preparations. These results indicated that neither intra- nor intermolecular disulfide bond was formed within BinA or between the neighboring BinA molecules. Since these residues are required for full toxicity, we propose that they may play a critical role during oligomerization or interaction between BinA and BinB to form the active complex.

We also have explored the role of cysteine on the protein folding and biological activity of BinB. Each of three cysteine residues at positions 67, 161, and 241 was substituted with either alanine or serine and investigated the effects of these replacements on the structural folding, and biological activity. Six mutants, C67A, C67S, C161A, C161S, C241A, and C241S, were generated. All of them were highly expressed as inclusion bodies at comparable levels as those of wild type. Biological activity assays revealed that C67A, C67S, C161A, and C161S significantly reduced the mosquito-larvicidal activity against *Culex quinquefasciatus* larvae whereas the mutation of C241 showed similar toxicity to the wild type (Table 2) suggesting that cysteine residues at positions 67 and 161 of BinB are critical for the toxicity. Intrinsic fluorescent spectrum analysis indicated that all mutants have similar conformation to the wild type protein (data not shown). SDS-PAGE analysis in the presence and absence of reducing agent showed similar profiles in the solubilized protein of both wild type and all mutants (data not shown). For the partially purified inclusions, however, the mobility of the major band corresponding to the BinB protein of wild type and all mutants was slightly faster in the sample without reducing agent (Fig. 6) suggesting that an intra-molecular disulphide bond may be

formed during inclusion formation. However, it seems that the observed intra-molecular disulfide bond from SDS-PAGE analysis was not correlated with the biological activity since the C241 mutants still retained their toxicity. Taken together, the dramatically reduced toxicity of the cysteine mutants especially at positions 67 and 161 of BinB may be due to the abolished ability of the mutant proteins to interact with BinA to form an active complex or to bind to receptor on the larval membrane.

3.5 Mutagenesis of charged residues in BinA and its effects on mosquito-larvicidal activity

Amino acid sequence alignment of BinA from various strains of *Bacillus sphaericus* shows major divergence in amino acid residues at positions 93, 99 and 104 [31;32]. Site-directed mutagenesis at these residues and binding assay revealed that position 93 plays an important role for the complex formation of the binary toxin [32] whereas mutations at residues 99 and 104 caused decrease in toxicity to mosquito larvae [31]. This finding leads to the suggestion that amino acid around this region (93 to 104) are essential for the mosquito-larvicidal activity and interaction with BinB. Complex formation between BinA and BinB is one of the toxicity determinant steps and ionic interactions may be one of the major forces involved in this complex formation. Therefore, the charged residues R97, E98, R101, and E114 were selected for alanine substitutions in this study.

Four BinA mutants, R97A, E98A, R101A, and E114A were generated. All of them were highly expressed as inclusion bodies at comparable levels as those of wild type. Intrinsic fluorescent spectrum analysis indicated that all mutants have similar conformation to the wild type protein (data not shown). Biological activity assays revealed that E98A, R101A, and E114A significantly reduced toxicity against *Culex quinquefasciatus* larvae whereas R97A abolished toxicity (Table 3) suggesting that these four charged residues are essential for the toxicity. The effect of these mutations on the interaction between BinA and BinB was investigated by dot blot analysis. Figure 7 shows that only the mutant R101A significantly reduced the binding ability to BinB component indicating that there is no correlation between the decrease toxicity of these BinA mutants and the loss of interaction to BinB. Therefore, the roles of these residues on the other steps involved in the mechanism of toxicity are required to be investigated further.

3.6 Proteolysis study of the binary toxin proteoliposomes by proteinase K for probing the fragments of proteins that insert into the membrane

From our previous experiments using infrared spectroscopy, we observed a 10% of H/D exchangeresistant amide protons (about 40 amino acids), but only BinB was found to insert in lipid monolayers (see above). Exhaustive proteolysis of liposome-associated BinA and BinB can reveal which part of the protein is inserted in membranes or simply tightly bound. BinA and BinB proteins were mixed separately with liposomes and followed by incubating with proteinase K to remove the part of protein that exposed to the solvent. The membrane-associated or membrane-inserted fragments could be protected from the proteinase K digestion. The proteinase K cleavage products were delipidated and analysed by SDS-PAGE. For BinB protein, a peptide with molecular mass about 30 kDa which may correspond to the membrane-embedded or membranebound domain was detected on the SDS gel (Fig. 8). This peptide has been sent for the amino acid sequence analysis and the mass will be determined by matrix assisted desorption ionization (MALDI). Once identified, this domain will be obtained separately by E. coli expression for further functional and structural studies. For BinA protein, no peptide band was detected after proteinase K digestion (data not shown) suggesting that BinA cannot insert into the membrane which is consistent with our previous report that BinA was unable to insert into the DMPC monolayer.

4. References

- 1. J.F.Charles, C.Nielson-LeRoux, and A.Delecluse *Annu. Rev. Entomol.* **41** (1996) 451-472.
- 2. P.Baumann, M.A.Clark, L.Baumann, and A.H.Broadwell *Microbiol. Rev.* **55** (1991) 425-436
- 3. P.Baumann, M.A.Clark, L.Baumann, and A.H.Broadwell *Microbiol. Rev.* **55** (1991) 425-436
- 4. A.G.Porter, E.W.Davidson, and J.W.Liu Microbiol. Rev. 57 (1993) 838-861.
- 5. E.W.Davidson, C.Oei, M.Meyer, A.L.Bieber, J.Hindley, and C.Berry *Can. J. Microbiol.* **36** (1990) 870-878.
- 6. L.Nicolas, A.Lecroisey, and J.F.Charles Can. J. Microbiol. 36 (1990) 804-807.
- 7. A.H.Broadwell and P.Baumann Appl. Environ. Microbiol. 53 (1987) 1333-1337.
- 8. P.Baumann, M.A.Clark, L.Baumann, and A.H.Broadwell *Microbiol. Rev.* **55** (1991) 425-436.
- 9. P.Baumann, M.A.Clark, L.Baumann, and A.H.Broadwell *Microbiol. Rev.* **55** (1991) 425-436.
- 10. C.Oei, J.Hindley, and C.Berry *J. Gen. Microbiol.* **138** (1992) 1515-1526.
- 11. C.Oei, J.Hindley, and C.Berry J. Gen. Microbiol. 138 (1992) 1515-1526.
- 12. M.H.Silva-Filha, C.Nielsen-Leroux, and J.F.Charles *Insect Biochem. Mol. Biol.* **29** (1999) 711-721.
- 13. I.Darboux, C.Nielsen-Leroux, J.F.Charles, and D.Pauron *Insect Biochem. Mol. Biol.* **31** (2001) 981-990.
- 14. E.W.Davidson, C.Shellabarger, M.Meyer, and A.L.Bieber *Can. J. Microbiol.* **33** (1987) 982-989.
- 15. J.F.Charles Ann. Inst. Pasteur Microbiol. 138 (1987) 471-484.
- 16. J.F.Charles Ann. Inst. Pasteur Microbiol. 138 (1987) 471-484.
- 17. C.Cokmus, E.W.Davidson, and K.Cooper J. Invertebr. Pathol. 69 (1997) 197-204.
- 18. J.L.Schwartz, L.Potvin, F.Coux, J.F.Charles, C.Berry, M.J.Humphreys, A.F.Jones, I.Bernhart, S.M.Dalla, and G.Menestrina *J. Membr. Biol.* **184** (2001) 171-183.

- 19. S.A.Tatulian *Biochemistry* **42** (2003) 11898-11907.
- 20. J.Torres, T.J.Stevens, and M.Samso Trends Biochem. Sci. 28 (2003) 137-144.
- 21. B.Promdonkoy, P.Promdonkoy, M.Audtho, S.Tanapongpipat, N.Chewawiwat, P.Luxananil, and S.Panyim *Curr. Microbiol.* **47** (2003) 383-387.
- 22. J.Torres, P.D.Adams, and I.T.Arkin J Mol. Biol. 300 (2000) 677-685.
- 23. D.M.Byler and H.Susi *Biopolymers* 25 (1986) 469-487.
- 24. Y.N.Chirgadze, O.V.Fedorov, and N.P.Trushina Biopolymers 14 (1975) 679-694.
- 25. D.Marsh J Mol. Biol. 297 (2000) 803-808.
- 26. C.Ege and K.Y.Lee *Biophys. J.* **87** (2004) 1732-1740.
- 27. E.Gazit, P.La Rocca, M.S.Sansom, and Y.Shai *Proc. Natl. Acad. Sci. U. S. A* **95** (1998) 12289-12294.
- 28. L.K.Tamm and S.A.Tatulian *Q. Rev. Biophys.* **30** (1997) 365-429.
- 29. D.Marsh J Mol. Biol. 297 (2000) 803-808.
- 30. L.Baumann, A.H.Broadwell, and P.Baumann J. Bacteriol. 170 (1988) 2045-2050.
- 31. C.Berry, J.Hindley, A.F.Ehrhardt, T.Grounds, S.de, I, and E.W.Davidson *J. Bacteriol.* **175** (1993) 510-518.
- 32. Z.M. Yuan, C.Rang, R.C.Maroun, V.Juarez-Perez, R.Frutos, N.Pasteur, C.Vendrely, J.F.Charles, and C.Nielsen-LeRoux *European Journal of Biochemistry* **268** (2001) 2751-2760.

5. Tables and Figures

Table 1. Mosquito larvicidal activity of the wild type and BinA mutant proteins against Culex quinquefasciatus larvae

BinB+	LC ₅₀ (ng/ml)	
BinA (wild type)	116 (66-164)	
BinA-C31A	inactive	
BinA-C31S	inactive	
BinA-C47A	inactive	
BinA-C47S	inactive	
BinA-C195A	840 (553-1,424)	
BinA-C195S	637 (488-821)	
BinA-C31A:C47A	inactive	
BinA-C31A:C195A	inactive	
BinA-C47A:C195A	inactive	
BinA-C31A:C47A:C195A	inactive	

Table 2. Mosquito larvicidal activity of the wild type and BinB mutant proteins against *Culex quinquefasciatus* larvae

BinA +	LC ₅₀ (ng/ml)		
BinB (wild type)	82 (34-124)		
BinB-C67A	inactive		
BinB-C67S	inactive		
BinB-C161A	inactive		
BinB-C161S	inactive		
BinB-C241A	44 (18-71)		
BinB-C241S	88 (39-142)		

Table 3. Motality rate of the wild type and BinA mutant proteins against $\it Culex$ $\it quinquefasciatus$ larvae at 50 $\mu g/ml$

Toxins (BinB +)	% Mortality±SEM
GST-BinA (wild type)	100.00±0.00
GST-R97A	3.33±2.33
GST-E98A	56.00±1.66
GST-R101A	86.60±2.03
GST-E114A	36.00±4.33

SEM=SD/ \sqrt{N}

N = Number of independent experiments, 3

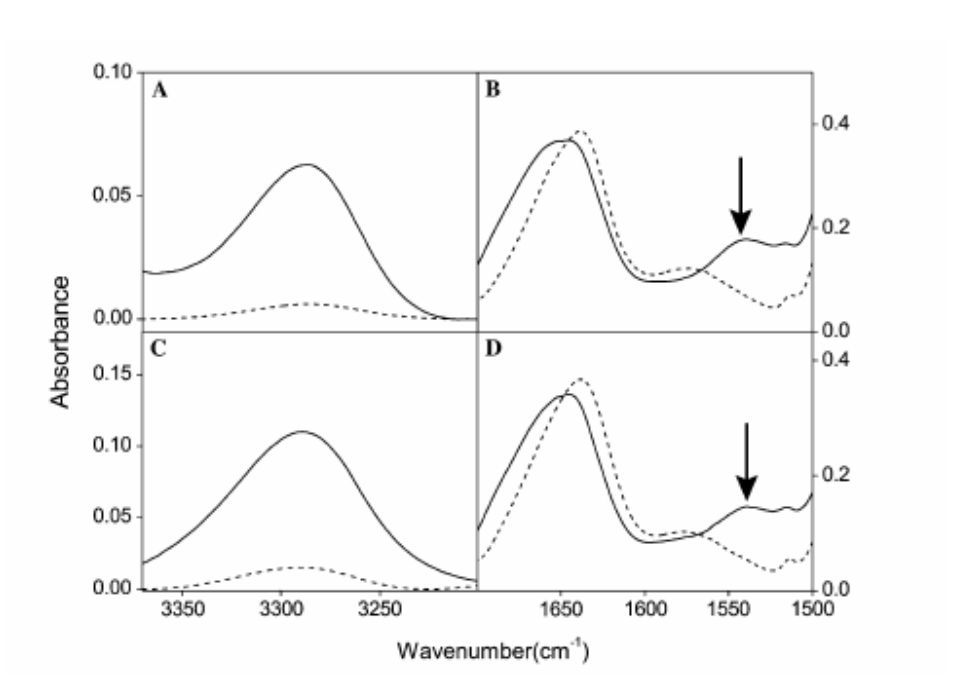


Figure 1. ATR-FTIR nonpolarized spectra of BinA and BinB in the presence of lipid bilayers. Amide A region (A) and amide I and II regions (B) in H2O (solid line) or in D2O (broken line) for BinA. The corresponding spectra for BinB are also shown (C and D).

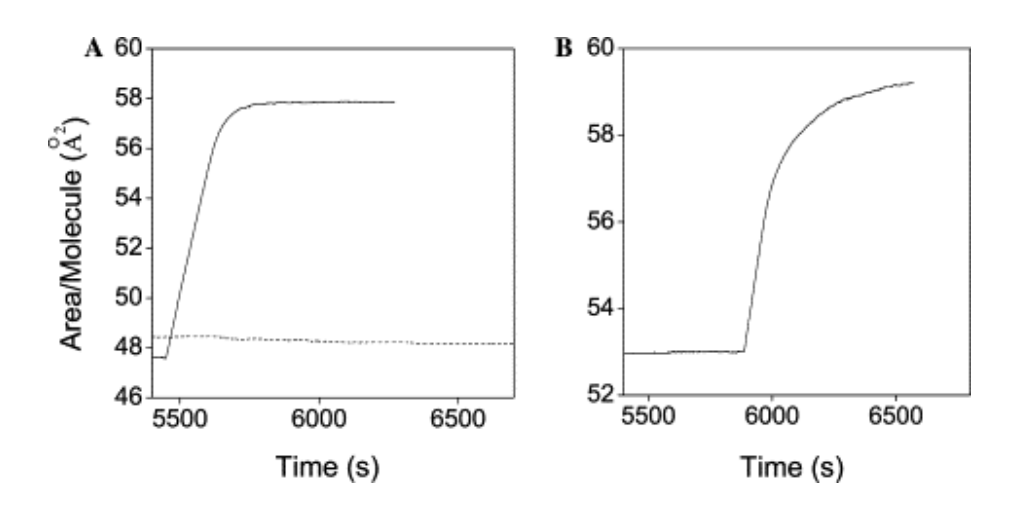


Figure 2. Insertion profile of BinA and BinB in DMPC monolayers. (A) BinA (broken line) and BinB (solid line); (B) equimolar mixture of BinA and BinB

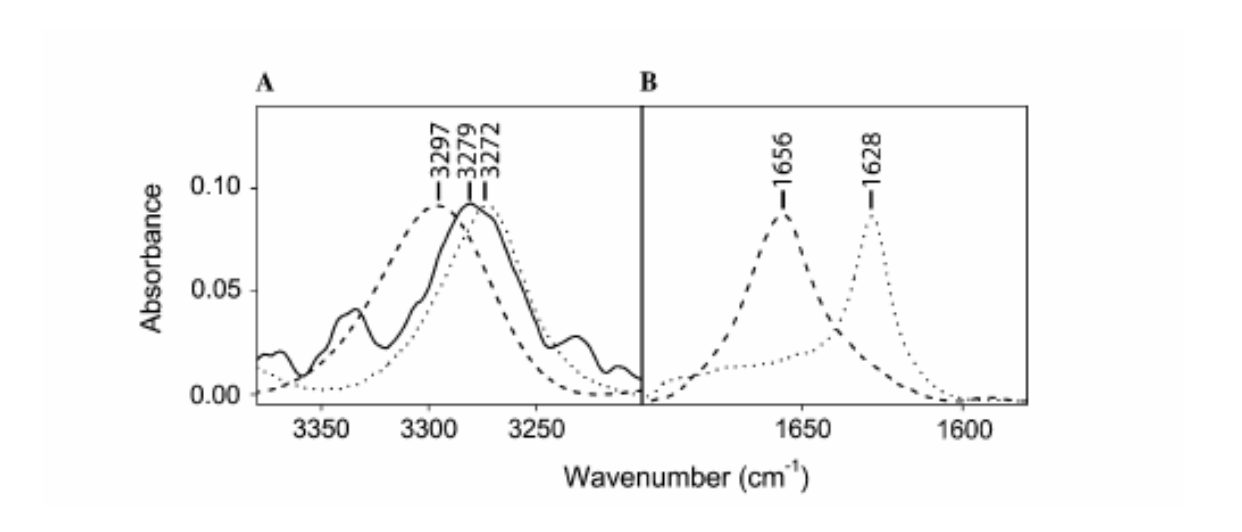


Figure 3 (A) Amide A region of the infrared spectrum in the presence of membranes after D_2O equilibration corresponding to the mixture BinA/BinB (solid line, maximum at 3279 cm⁻¹), a synthetic transmembrane α-helical peptide from αIIb integrin (broken line, maximum at 3297 cm⁻¹) and a α7 peptide from a Cry4Ba toxin, which adopts β structure (dotted line, maximum at 3272 cm⁻¹). (B) amide I spectra of the α-helical αIIb integrin (maximum at 1656 cm⁻¹) and β structured α7 peptide (maximum at 1628 cm⁻¹).

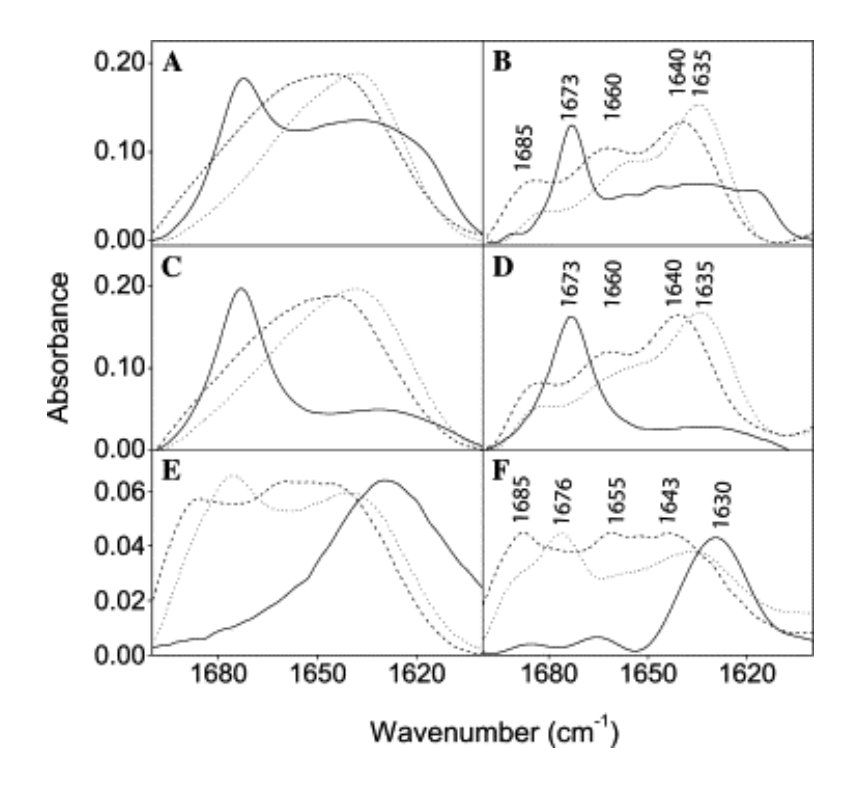


Figure 4. Amide I region for the original infrared spectra (left column) of BinA, BinB, and mixture BinA/BinB in the presence or absence of membranes. The corresponding deconvoluted spectra are shown in the right column. The spectra correspond to toxin BinA, BinB, and BinA/BinB are shown in (A), (C), and (E), respectively. Spectra were obtained either in D_2O aqueous solution (solid line), or in the presence of DMPC lipid bilayers equilibrated in H_2O (broken line) or D_2O (dotted line). The positions of the main bands are indicated in the deconvoluted spectra (B, D, and F).

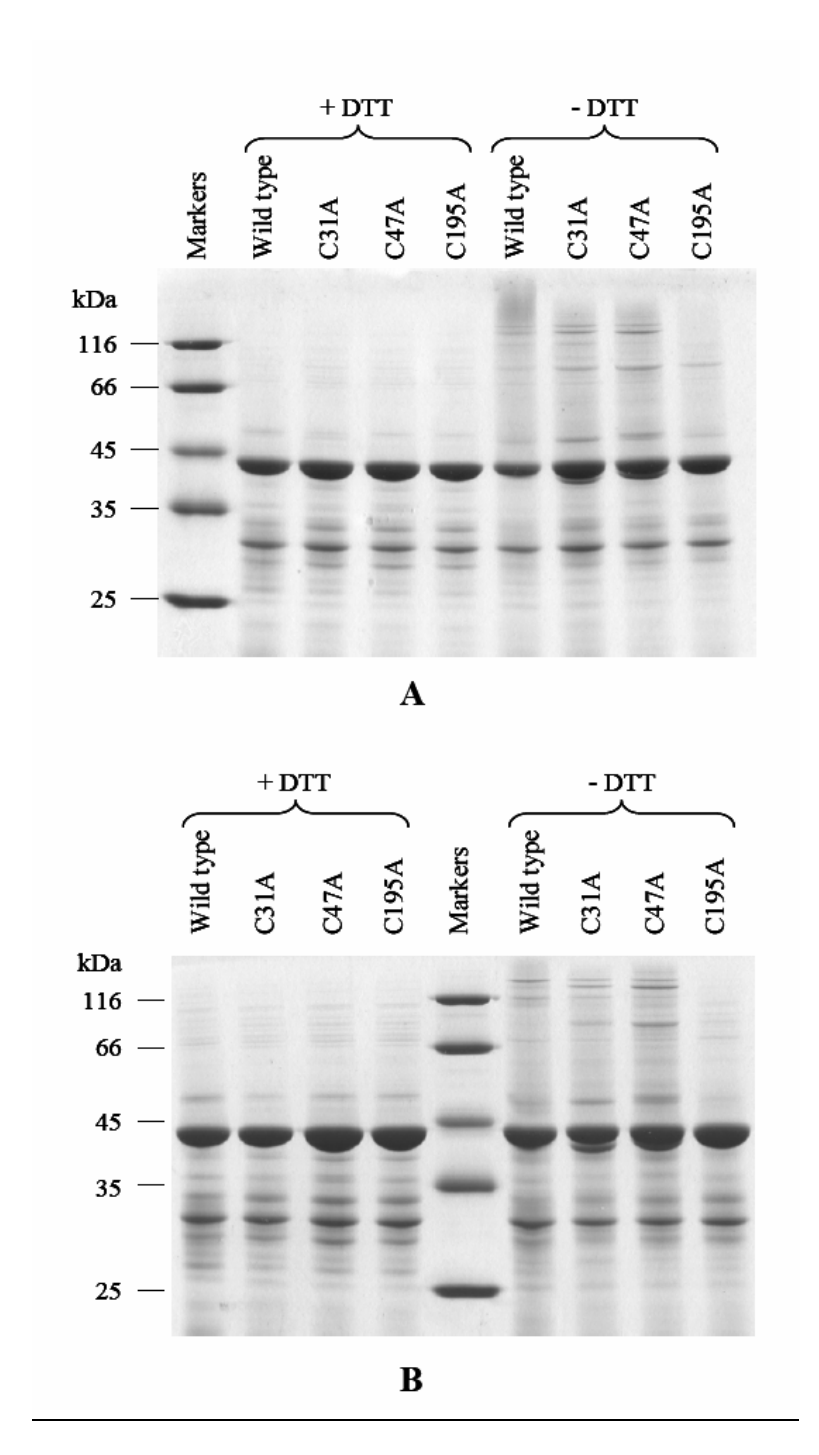


Figure 5. SDS-PAGE of BinA and its mutants in the presence and absence of reducing agent (10 mM DTT)

Inclusion bodies (A) and solubilized proteins (B) were mixed with SDS-PAGE sample buffer with or without reducing agent (+DTT or –DTT). The mixtures were boiled for 10 minutes before loaded in each lane. The mutant proteins C31S and C47S showed similar pattern to C31A and C47A whereas C195S, all double and triple mutants showed similar pattern to C195A.

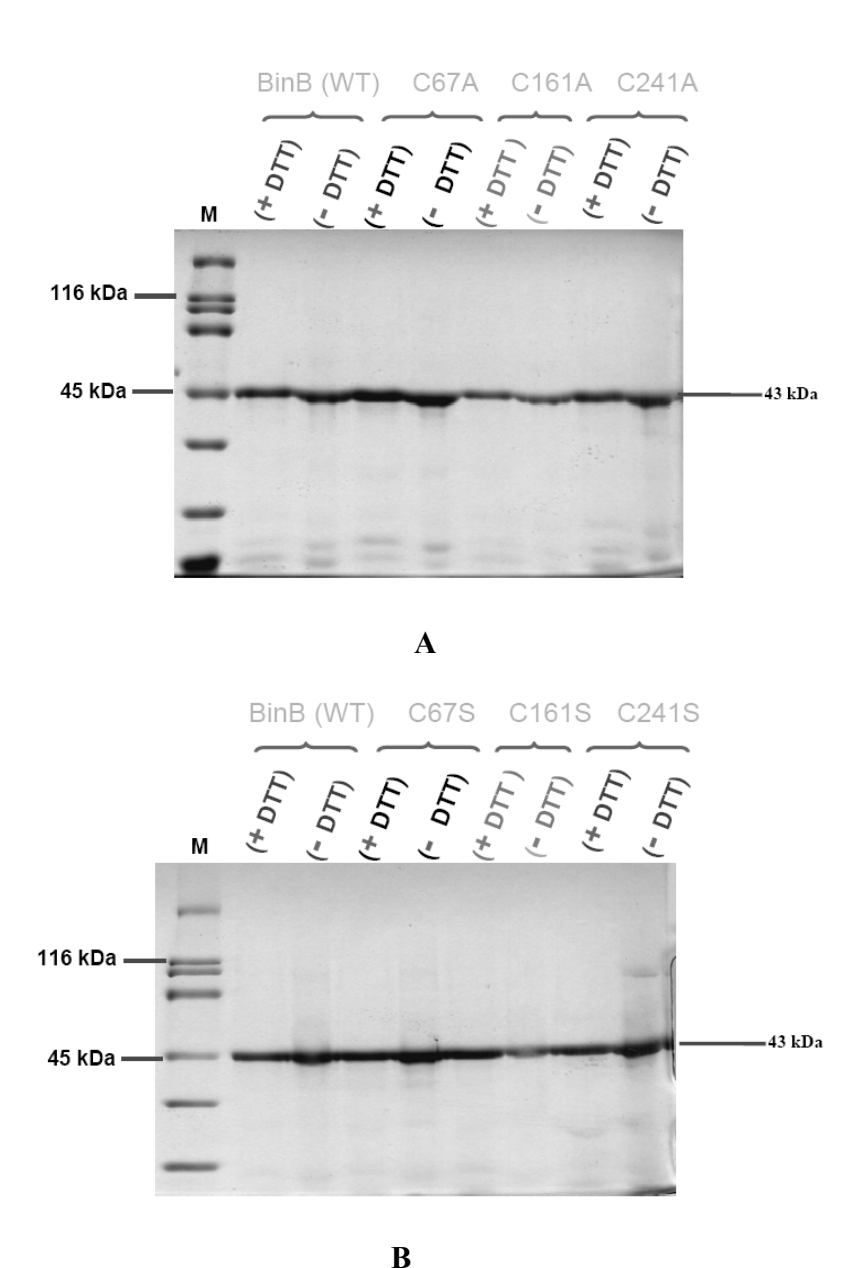


Figure 6. SDS-PAGE of BinB and its mutants in the presence and absence of reducing agent (10 mM DTT)

Inclusion bodies of BinB and its mutants were mixed with SDS-PAGE sample buffer with or without reducing agent (+DTT or -DTT). The mixtures were boiled for 10 minutes before loaded in each lane. The mutant proteins C67A, C161A and C241A (A) showed similar patterns with the reduced-mobility bands in the samples with reducing agent whereas the mutant proteins C67S, C161S and C241S (B) showed no difference in the mobility of bands with or without reducing agent.

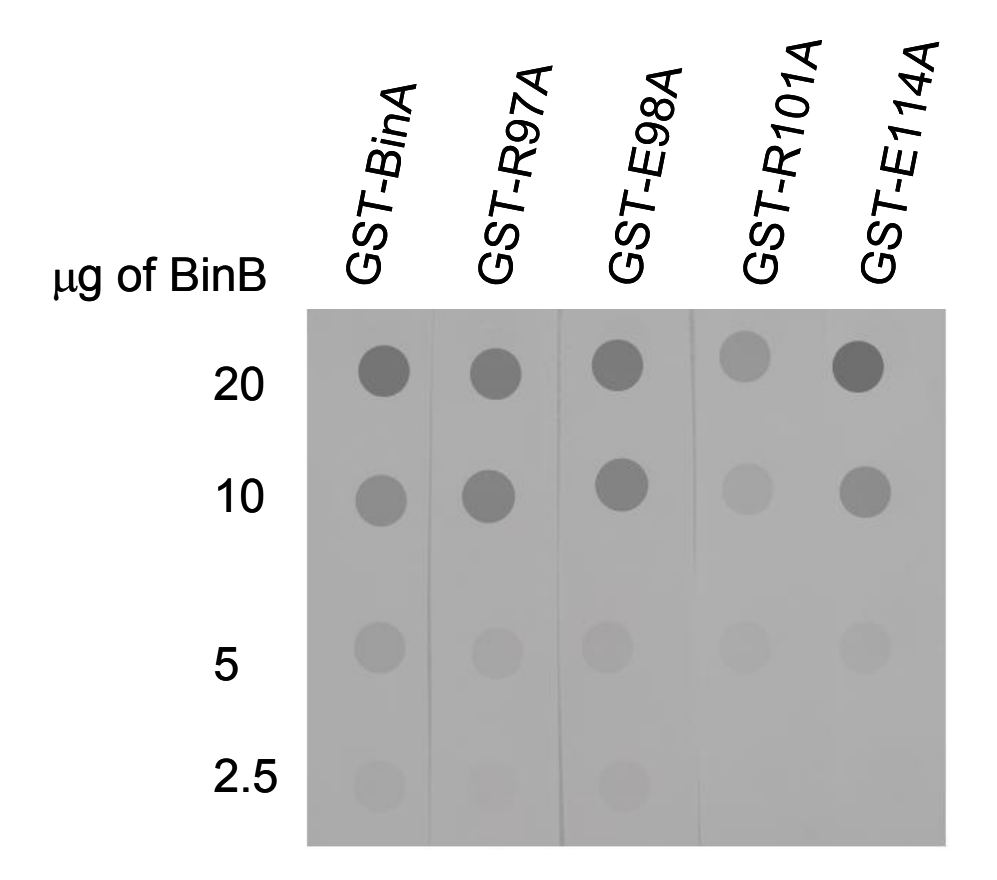


Figure 7. The Interaction between BinB and BinA or its mutants

BinB protein was immobilized onto PVDF membrane by dot blot. The immobilized BinB on the membrane was then overlaid with GST-BinA or its mutants. The reactive signals were detected by probing with a specific antibody against GST.

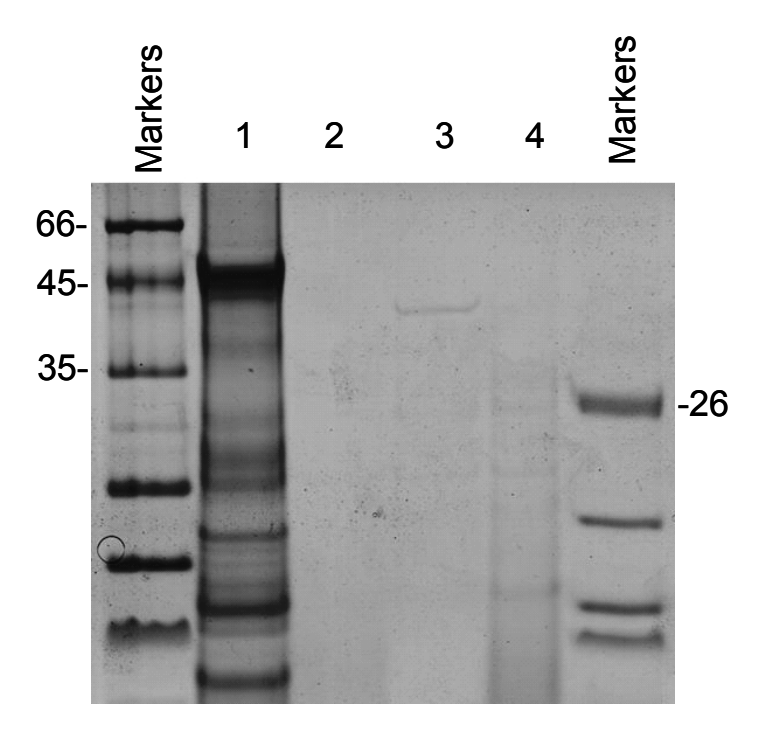


Figure 8. Proteolysis of the binary toxin proteoliposomes by proteinase K

BinB protein was mixed with liposomes and followed by incubating with proteinase K to remove the part of protein that exposed to the solvent. The membrane-associated or membrane-inserted fragments protected from the proteinase K digestion were delipidated and analysed by SDS-PAGE. Lane 1 shows the BinB protein. Lanes 2 and 3 were the BinB protein cleaved by proteinase K in the absence and presence of liposomes, respectively. Lane 4 was the digested products in the soluble fraction.

6. ผลงานวิจัยที่ตีพิมพ์ในวารสารวิชาการระดับนานาชาติ

- **6.1 Boonserm, P.**, Moonsom, S., Boonchoy, C. Promdonkoy, P., Parthasarathy K. and Torres, J. (2006). Association of the componenents of the binary toxin from *Bacillus sphaericus* in solution and with lipid bilayers. *Biochem. Biophys. Res. Commun.* 342, 1273-8. Impact factor 2.855.
- **6.2** Promdonkoy, B., Promdonkoy, P., Chaisalee, B., **Boonserm, P.** and Panyim, S. (2007). Cys31, Cys47 and Cys195 in BinA are essential for toxicity of a binary toxin from *Bacillus sphaericus*. *Curr. Micorbiol*. (submitted). Impact factor 1.007
- **6.3** Sanitt, P., **Boonserm, P**., Panyim, S. and Promdonkoy, B. (2007). Role of charged amino acid residues on the mosquito-larvicidal activity of BinA from *Bacillus sphaericus*. (manuscript in preparation for submission to *Curr. Micorbiol.*, Impact factor 1.007)



Available online at www.sciencedirect.com





Biochemical and Biophysical Research Communications 342 (2006) 1273-1278

www.elsevier.com/locate/vbbrc

Association of the components of the binary toxin from Bacillus sphaericus in solution and with model lipid bilayers

Panadda Boonserm ^{a,*}, Seangduen Moonsom ^a, Chanikarn Boonchoy ^b, Boonhiang Promdonkoy ^c, Krupakar Parthasarathy ^d, Jaume Torres ^{d,*}

^a Institute of Molecular Biology and Genetics, Mahidol University, Salaya, Phuttamonthol, Nakornpathom 73170, Thailand b Institute of Science and Technology for Research and Development, Mahidol University, Salaya, Phuttamonthol, Nakornpathom 73170, Thailand ^c National Center for Genetic Engineering and Biotechnology, National Science and Technology Development Agency, 113 Paholyothin Road, Klong 1, Klong Luang, Pathumthani 12120, Thailand ^d School of Biological Sciences, Nanyang Technological University, 60 Nanyang Drive 637551, Singapore

> Received 24 January 2006 Available online 24 February 2006

Abstract

We show herein that interaction in aqueous solution of the two components of binary toxin from Bacillus sphaericus, BinA and BinB, leads to a dramatic conformational change, from \(\beta \) turns or random coil, to \(\beta \) structure. Also, either BinA or BinB separately or their equimolar mixture, interact with lipid bilayers resulting in further conformational changes. Upon membrane association, the change in conformation observed for BinA or BinB separately is different from that observed when the proteins are combined, indicating that proper folding depends on the presence of the complementary subunit. We also show, in contrast to previous reports, that BinB, but not BinA, is able to insert in model neutral lipid monolayers. © 2006 Elsevier Inc. All rights reserved.

Keywords: Infrared spectroscopy; Binary toxin; Membranes; Mechanism; Insertion; Circular dichroism

Many strains of Bacillus sphaericus (Bs) produce a binary toxin which is highly active against the larvae of *Culex* and Anopheles mosquitoes. The same toxin, however, is only mildly toxic or nontoxic to Aedes [1]. This toxin is composed of two proteins, 42 kDa (BinA) and 51 kDa (BinB), which are deposited as parasporal crystals during sporulation [2]. Both proteins are required for larvicidal activity, and maximal toxicity is observed when they are present in equimolar amounts [2,3], although at high concentrations, even BinA alone can be toxic to cultured Culex cells [2,4-6].

After the crystal toxins are ingested by the susceptible larvae, crystalline inclusions are solubilized in the alkaline pH of the larvae midgut, followed by activation by larval proteases, and binding of toxin proteins to the gastric cecum and posterior midgut [2]. It has been demonstrated that BinB is the primary binding component, and directs the localized binding of BinA [7]. Subsequent internalization of the binary toxin following binding has been observed, and it has been suggested to be correlated with toxicity [7]. In Culex pipiens larvae, the putative receptor has been identified as α-glucosidase [8] and this receptor has been cloned [9]. However, the detailed mechanism that leads to the death of mosquito larvae, after binding of the toxin complex, is not clearly understood.

Ultrastructural observations [10,11] have profound morphological changes of the larval midgut

^{*} Abbreviations: ATR-FTIR, attenuated total reflection Fourier transform infrared spectroscopy; DMPC, dimyristoylphosphocholine; Bs, Bacillus sphaericus; Bt, Bacillus thuringiensis; IPTG, isopropyl-β-D-thiogalactopyranoside; FPLC, fast performance liquid chromatography; DTT, dithiothreitol; FWHH, full width at half-height.

Corresponding authors. Fax: +66 2441 9906 (P. Boonserm), +65 6791 3856 (J. Torres).

E-mail addresses: mbpbs@mahidol.ac.th (P. Boonserm), jtorres@ntu. edu.sg (J. Torres).

epithelial cells. Also, electrophysiological studies conducted on cultured *Culex quinquefasciatus* cells have provided evidence that the activated binary toxin, like *Bacillus thuringiensis* (Bt) toxins, interacts with cell membranes and may form pores [12]. Support for binary toxin-induced membrane permeabilization has been provided by a study of channel activity and membrane permeability using a receptor-free planar lipid bilayer and large unilamellar phospholipid vesicles. In this study, BinA, and to a lesser extent BinB, were suggested to increase permeability [13].

Despite these initial studies, structural information on this system, both in terms of secondary and tertiary structure, is lacking. Crucially, the structural changes that may take place simultaneously with membrane association and dimer formation and possibly oligomerization have not been studied. Infrared spectroscopy is specially suitable for the study of membrane proteins [14,15] and, especially, to monitor structural changes that take place in facultative membrane proteins during the transition from aqueous solution to the membrane environment. Therefore, to provide further insight into the interaction of the binary toxin components with lipid membranes, we have investigated their secondary structure in the absence and in the presence of lipids, using attenuated total reflection Fourier transform infrared spectroscopy (ATR-FTIR). We have also monitored the membrane insertion of each of these components in a model lipid monolayer. Our results clearly demonstrate that the interaction of the binary toxin components with the lipid membrane is accompanied by a dramatic conformational change.

Materials and methods

Protein preparation. Escherichia coli BL21 (DE3) pLysS clones harboring the recombinant plasmids [16] were grown at 37 °C in a Luria-Bertani medium containing 100 μg/ml ampicillin and 34 μg/ml chloramphenicol until OD600 of the culture reached 0.3-0.5. Protein expression was induced with isopropyl-β-D-thiogalactopyranoside (IPTG) at a final concentration of 0.1 mM. The culture was further incubated at 37 °C for 5 h. E. coli cultures overexpressing the binary toxin as cytoplasmic inclusions were harvested by centrifugation and resuspended in phosphate buffer (100 mM KH₂PO₄, pH 6.5) and suspended cells were then disrupted by three times of French press at 10,000 psi. After centrifugation at 10,000g, 4 °C for 15 min, the pellet was resuspended in phosphate buffer containing 0.1% Triton X-100, 0.83% NaCl and incubated on ice for 30 min. After centrifugation, protein inclusions were further washed once with phosphate buffer and two times with distilled water. Protein concentrations of the partial-purified inclusions were determined by using a protein microassay reagent (Bio-Rad), with a bovine serum albumin fraction V (Sigma) as a standard. Inclusions (1–2 mg/ml) were solubilized by incubation at 37 °C for 1 h in 25 mM NaOH, 5 mM DTT. Solubilized protoxins were then separated from insoluble materials by using centrifugation at 12,000g for 15 min. Soluble protein was stepwise dialyzed in carbonate buffer (50 mM Na₂CO₃, pH 10.0) and concentrated by using ultrafiltration at 4 °C using a Centriprep column (30-kDa cutoff, Amicon). The protein was further purified by a size-exclusion FPLC system (Superose 12 HR 10/30, Amersham Pharmacia Biotech) with a linear gradient of 50 mM Na₂CO₃, pH 10.0, 1 mM DTT at a flow rate of 0.4 ml/ min. Eluted fractions containing the purified protein were pooled and concentrated to 3-5 mg/ml by ultrafiltration as described above. The purified proteins were kept at -20 °C.

Protocol for ATR-FTIR. Infrared spectra were recorded on a Nicolet Nexus spectrometer (Madison, USA) purged with N_2 and equipped with a MCT/A detector, cooled with liquid nitrogen. Attenuated total reflection (ATR) spectra were measured with a 25-reflection ATR accessory from Graseby Specac (Kent, UK) and a wire grid polarizer (0.25 μ m, Graseby Specac). A total of 200 interferograms collected at a resolution of 4 cm⁻¹ were averaged for every sample and processed with 1 point zero filling and Happ-Genzel apodization.

Incorporation of the protein to DMPC bilayers. Sample preparation was performed essentially as described previously [17]. Initially, DMPC was solubilized in ethanol and dried after exposure to air. The purified protein was added to the dry lipid in 50 mM sodium carbonate buffer, pH 10, at a concentration of 1 mg/ml. The total lipid (DMPC):protein molar ratio was 100:1. Approximately 100 μ l of this solution, containing protein in the presence of multilamelar liposomes, was deposited in successive aliquots of 10 μ l onto a trapezoidal (50 mm \times 2 mm \times 20 mm) Ge internal reflection element (IRE). Bulk water was removed using a dry N_2 stream through the ATR compartment to form regular stacks of lipid bilayers parallel to the internal reflection element surface. For transmission experiments, the protein dissolved in buffer was previously lyophilized and later solubilized with 100 μ l D2O. This solution was transferred to a rectangular transmission cell with CaF2 windows.

Infrared data analysis. The secondary structure composition of (i) BinA, (ii) BinB, and (iii) the mixture BinA/BinB at 1:1 molar ratio was obtained by analysing the amide I band and using previous assignments [18]. Main bands were identified after mild Fourier deconvolution (FWHH 20 cm⁻¹ and k 1.5) and curvefitted to obtain component bands after subtracting the contribution of amino acid side chain absorption to the amide I [19]. The spectrum in the amide I region corresponding to the side chains was subtracted from the experimental amide I until the band corresponding to protonated tyrosine, at 1515 cm⁻¹, was eliminated. Dichroic ratios were calculated as the ratio between the integrated absorptions of the spectra collected with parallel and perpendicular polarized light. Isotopic exchange (Hydrogen /Deuterium, H/D) was calculated from the ratio Amide II/Amide I before and after exchange, using the nonpolarized spectra. Nonpolarized spectra were obtained from the parallel (||) and perpendicularly (\pm) ATR polarized spectra, using the expression 1 (\parallel) + 1.44 (\perp) as described previously [20].

Preparation of LB monolayers. The interaction of BinA and BinB with DMPC lipid monolayers was monitored using a constant surface pressure assay [21] using a NIMA Langmuir–Blodgett (LB) trough 611 (Coventry, UK). Before starting the experiment, the trough was cleaned successively with chloroform or ethanol, followed by rinsing with deionized water. Carbonate buffer, pH 10.0, was used as the subphase. DMPC dissolved in chloroform was spread on the surface of the buffer. After 15–20 min, the monolayer was compressed at a speed of 10 cm²/min, until the surface pressure reached 25 mN/m. Control injections containing only buffer were delivered into the subphase before each experiment. The sample containing the protein was then injected (3–5 nmoles) through an L-shaped syringe from underneath the Teflon barrier. All experiments were performed at room temperature.

Dynamic light scattering measurements. Dynamic Light Scattering (DLS) measurements were performed using a 90 Plus particle size analyzer (Brookhaven Instruments Corp).

Results and discussion

Amide proton exchange

To determine the percentage of proton exchange resistant amide groups, we exposed the purified protein samples (Fig. 1) to D_2O (see Materials and methods), and monitored the changes in intensity in the bands amide II and amide A. Fig. 2 shows that when BinA or BinB was reconstituted in the presence of liposomes, the amide II band

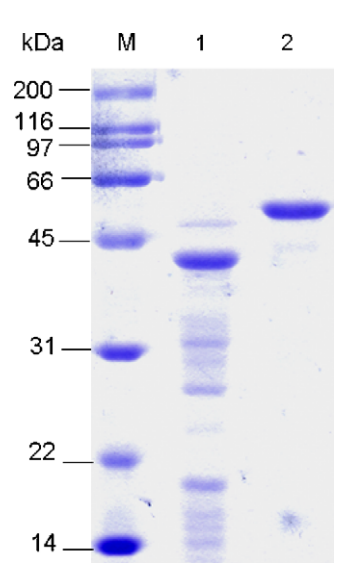


Fig. 1. Coomassie-stained SDS-PAGE (12% gel) showing the size-exclusion purified protein of BinA (lane 1) and BinB (lane 2). M represents molecular mass standards.

(N-H bending) at $\sim 1550~\rm cm^{-1}$ disappeared after D_2O equilibration (see arrows in Figs. 2B and D) suggesting complete exchange. However, inspection of the amide A, due to N-H stretching, (Figs. 2A and C, dotted line), showed a small band representing nonexchanged amide protons. The area of this remaining band corresponds to approximately 10% of the total amide A before deuterium exchange (shown in Figs. 2A and C, solid line). This percentage corresponds to approximately 40 amino acids. A similar percentage for this residual amide A was obtained for BinA, BinB or the mixture BinA/BinB (not shown).

The lack of complete exchange does not necessarily imply partial insertion in the membrane, and it could be originated by simple membrane association, or the presence of slow-exchanging secondary structures.

Langmuir-Blodgett trough

To distinguish between those above possibilities, we performed experiments using a Langmuir-Blodgett trough. Fig. 3 shows that when BinA or BinB was injected in the subphase of the trough, only BinB inserted in the DMPC monolayer (Fig. 3A, solid line). When BinA and BinB were mixed and added to the subphase (Fig. 3B), insertion was also observed, and to the same extent as that observed for BinB alone, although with different kinetics. The fact that the extent of insertion was the same for BinB and the mixture BinA/BinB suggests that in both cases only BinB inserts. The kinetics are however affected by the presence of BinA, which probably induces conformational changes in BinB. The difference in behavior between BinA and BinB is consistent with their suggested separate roles in vivo [7], with only BinB being responsible for binding to a membrane receptor. Our results, however, are in contrast with those reported by Schwartz et al. [13], who suggested more efficient pore formation for BinA than for BinB based on calcein permeabilization experiments. In the latter results, however, the effect of permeabilization by detergent-like activity, as opposed to pore formation, of the toxins cannot be discarded. Our data, in contrast are direct and show conclusively that only BinB, and not BinA, inserts in a DMPC monolayer. Therefore, the reason for the presence of nonexchanged amide protons in BinB is due, at least partly, to membrane insertion. Those for BinA, in contrast, could be due to membrane association or nonexchanging secondary structure.

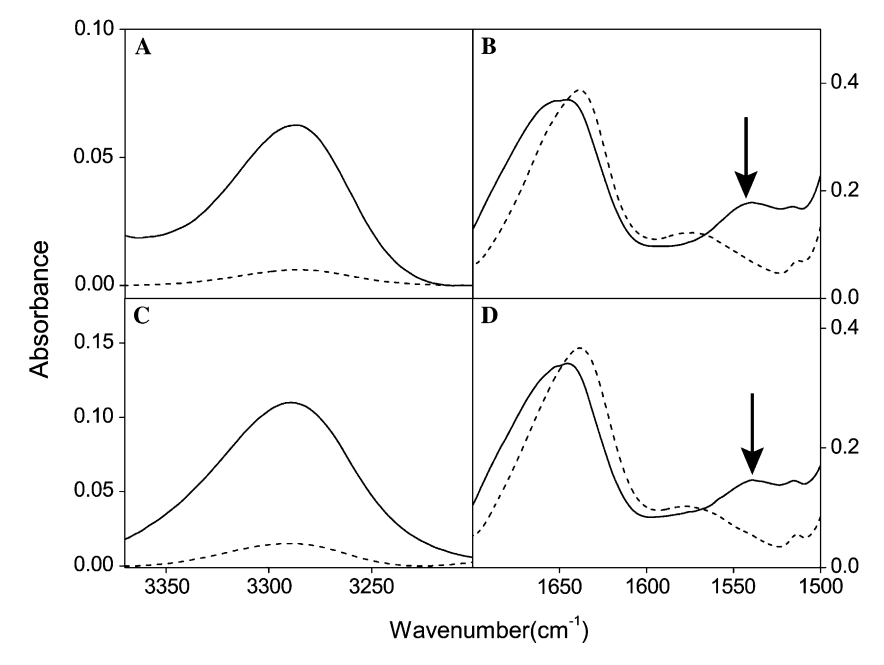


Fig. 2. ATR-FTIR nonpolarized spectra of BinA and BinB in the presence of lipid bilayers. Amide A region (A) and amide I and II regions (B) in H_2O (solid line) or in D_2O (broken line) for BinA. The corresponding spectra for BinB are also shown (C and D).

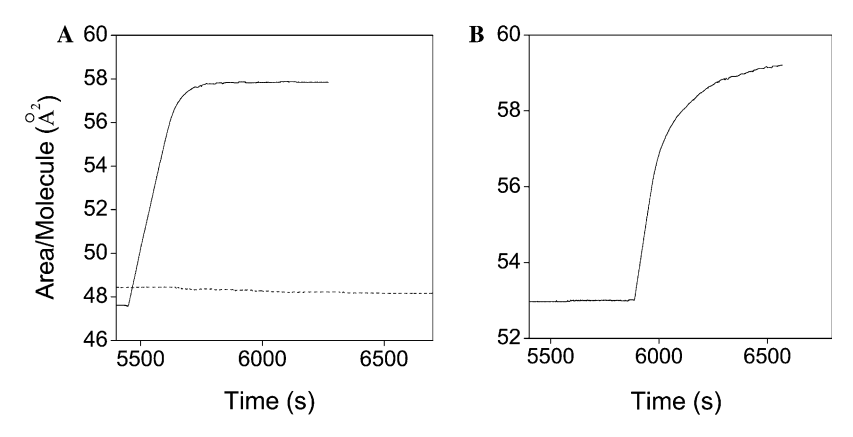


Fig. 3. Insertion profile of BinA and BinB in DMPC monolayers. (A) BinA (broken line) and BinB (solid line); (B) equimolar mixture of BinA and BinB.

The membrane inserted residues in BinB, which only constitute a 10% of the total (see above), could be inserted as α -helices, forming an α -helical hairpin, similar to those described for Cry toxins [22]. Alternatively, oligomerization of the toxins could lead to the formation of a transmembrane β-barrel, which could also explain a pore behavior. To examine these two possibilities, we used the fact that the amide A frequency is sensitive to secondary structure, and shifts towards higher frequencies for α-helical structures, reflecting the presence of weaker hydrogen bonds than those found in β -sheets [23]. Therefore, we examined the frequency of amide A in the mixture BinA/BinB in the presence of lipid bilayers, after D₂O equilibration (Fig. 4A). In these conditions, the amide A only corresponds to the part of the protein that is inserted in the membrane. We then compared the frequency of this band to that of peptides known to adopt either a completely α -helical or β structural conformation (see Fig. 4, legend). The secondary structure of these model peptides is either α -helical, with amide I centered at 1656 cm⁻¹ or β-structure, with amide I centered at 1628 cm⁻¹, respectively (shown in Fig. 4B). Fig. 4A shows that the amide A corresponding to the protected residues in the mixture BinA/BinB (Fig. 4A, solid line) is similar to that of the peptide that adopts a β structure

(Fig. 4A, dotted line), suggesting that the protected residues in BinA/BinB are mostly in a β -sheet conformation. Consistent with the monolayer insertion data (see above), the frequency for the residual amide A in BinB was almost superimposable to that of the mixture BinA/BinB (not shown). For BinA, which showed no insertion (Fig. 3), the amide A was broader and centered between that of the α and β model peptides (not shown).

Overall, this suggests that the membrane inserted residues in BinB and BinA/BinB adopt a β -sheet conformation, not α -helical, suggesting that the putative pores formed by this binary toxin consist of β -barrels. Further, the dichroic ratio for the amide A was $1.9\pm0.1,$ which is compatible with typical β -barrel dichroic ratios [20].

Conformational change after membrane association

In proteins, the amide I region of the infrared spectrum is sensitive to the secondary structure content. Fig. 5 shows the amide I region for BinA, BinB and their mixture, both in solution and in the presence of lipid bilayers. In solution, and in all cases, the amide II band was absent (not shown), suggesting a total, or almost complete, exchange of the amide protons. For BinA, in aqueous solution, i.e., in the

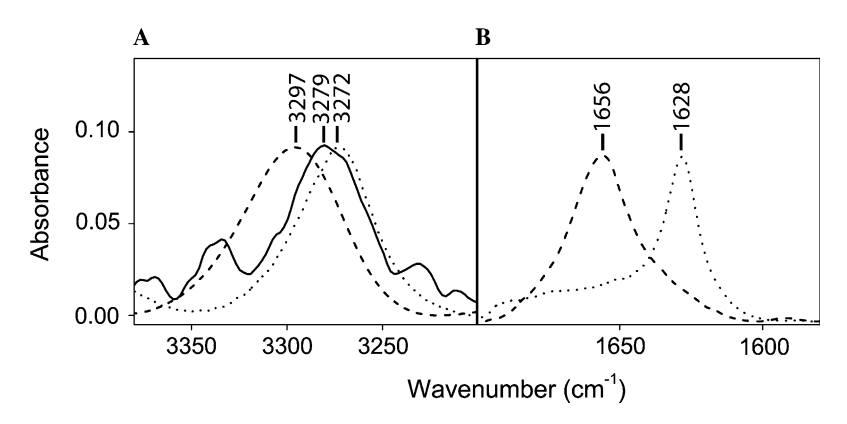


Fig. 4. (A) Amide A region of the infrared spectrum in the presence of membranes after D_2O equilibration corresponding to the mixture BinA/BinB (solid line, maximum at 3279 cm⁻¹), a synthetic transmembrane α -helical peptide from α IIb integrin (broken line, maximum at 3297 cm⁻¹), and an α 7 peptide from a Cry4Ba toxin, which adopts β structure (dotted line, maximum at 3272 cm⁻¹). (B) Amide I spectra of the α -helical α IIb integrin (broken line, maximum at 1656 cm⁻¹) and β structured α 7 peptide (dotted line, maximum at 1628 cm⁻¹).

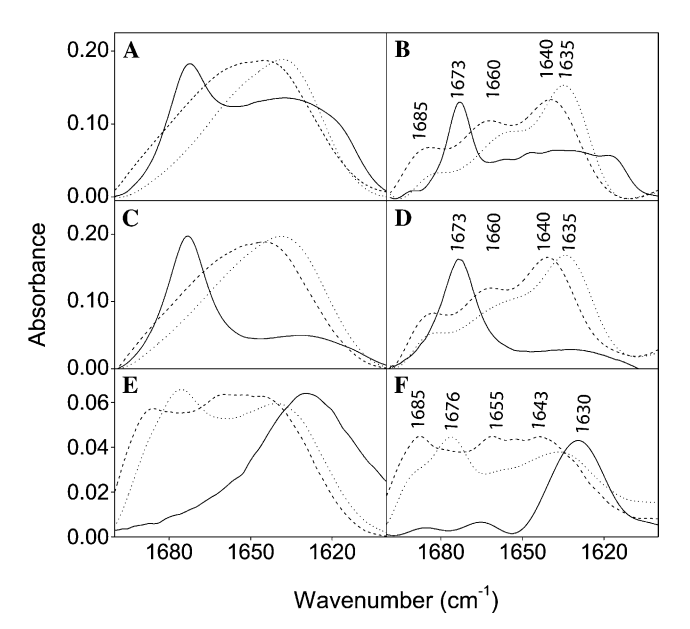


Fig. 5. Amide I region for the original infrared spectra (left column) of BinA, BinB, and mixture BinA/BinB in the presence or absence of membranes. The corresponding deconvoluted spectra are shown in the right column. The spectra correspond to toxin BinA, BinB, and BinA/BinB are shown in (A), (C), and (E), respectively. Spectra were obtained either in D_2O aqueous solution (solid line), or in the presence of DMPC lipid bilayers equilibrated in H_2O (broken line) or D_2O (dotted line). The positions of the main bands are indicated in the deconvoluted spectra (B, D, and F).

absence of membranes, the amide I shows an intense band at 1673 cm^{-1} (Fig. 5A, solid line) that we assign to β -turns (see Materials and methods). We should point out, however, that model calculations [24] have shown that contribution of non α and non β sheet (i.e., random structures and β-turns) can spread over a wide range of the amide I band, therefore a substantial component of random structure for these spectra in solution cannot be discarded. In contrast, when BinA was prepared in the presence of lipid bilayers in bulk H₂O (Fig. 5A, broken line), a more heterogeneous spectrum was observed, with features at 1685, 1660, and 1640 cm⁻¹ (see deconvoluted spectra in Fig. 5B), with most of the intensity in the latest band (1640 cm⁻¹), that we assign to β strands. When this sample was equilibrated in D₂O (Fig. 5A, dotted line), a small shift was observed in all the amide I bands, consistent with amide proton exchange. A similar behavior was observed for BinB (Figs. 5C and D), although in solution (Fig. 5C, solid line), the spectrum appears more homogeneous than for BinA, with almost no features below 1660 cm⁻¹.

These data clearly show, therefore, that interaction of either BinA or BinB with lipid bilayers results in a dramatic conformational change that involves not only changes in tertiary structure, but even variations in secondary structure that affect most of the molecule. A more detailed quantification of the band contributions to the amide I is shown in Table 1.

Fig. 5E (solid line) shows that the mixture BinA/BinB, either in solution or in the absence of membranes, is *not*

Table 1 Percentages of secondary structure calculated from the amide I envelope for the BinA and BinB subunits after exposure to D_2O , either in the presence of DMPC lipid bilayers or in aqueous solution

Protein	β Strands	α Helix	β Turns
BinA-DMPC	68	19	13
BinA-solution	44	20	36
BinB-DMPC	55	15	30
BinB-solution	36	13	51
BinA/BinB-DMPC	41	15	44

Bands centered in the interval 1690–1660, 1660–1645, and 1645–1610 cm⁻¹ were assigned to β -turns, α -helix, and β -structure, respectively.

a sum of the spectra for BinA and BinB in the same conditions, therefore BinA and BinB interact when they are in aqueous solution, i.e., before their interaction with lipid bilayers. The spectrum of this mixture in solution shows a band at 1630 cm⁻¹ which we assign to β structure. No other features are observed in the amide I. Further, when the mixture BinA/BinA interacts with membranes (Fig. 5E, broken line and dotted line), the spectrum suffers a dramatic change. In the presence of membranes exposed to H₂O (Fig. 5E, broken line), the band at 1630 cm⁻¹ disappears and other bands are observed. One of these additional bands is centered at 1685 cm⁻¹ and, upon exposure to D₂O (Fig. 5E, dotted line), it shifts to 1676 cm⁻¹, which is similar to the band observed when BinA or BinB is in D₂O solution. This clearly shows that the end product of the folding elicited by contact of either BinA or BinB with the membrane is not the same as that observed for the mixture BinA/BinB. When the latter species binds to the membrane, the resulting structure contains elements of the individual proteins in solution and in a membrane-bound state.

In this respect, dynamic light scattering analysis showed that both BinA and BinB separately, and the equimolar mixture of BinA and BinB, oligomerize in solution, and this oligomerization increases with time at room temperature over many minutes, but does not produce precipitation within this time interval (not shown). A previous report also showed oligomerization of BinA and BinB in solution [25].

Prediction of secondary structure using Profile network prediction Heidelberg (PROF) [26] for BinB gives 7% helix (H), 37% β strands (E), and 55% of either random or β turns or loops (L), which is in general consistent with our experimental results. For BinA, the prediction was 2%, 48%, and 50% for H, E, and L, respectively.

Overall, our results indicate that BinA and BinB interact in solution before binding to a specific or nonspecific receptor. Also, only BinB appears to be involved in membrane insertion, although both proteins associate to the lipid bilayer experiencing a dramatic conformational change. Fig. 6 shows a schematic model derived from the various spectral changes observed in this work. The folding observed for the membrane associated form of BinA or BinB is clearly different from that observed for BinA/BinB,

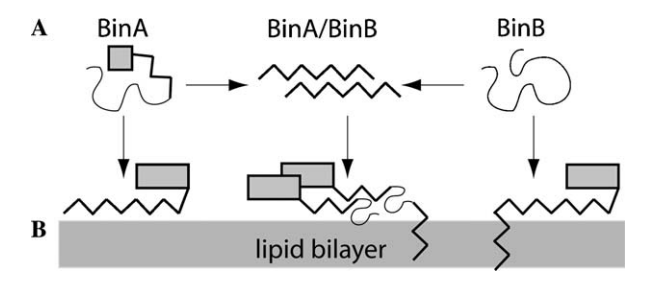


Fig. 6. Scheme of the structural changes of BinA, BinB, and their equimolar mixture in solution (A) or after association to lipid bilayers (B), based on the spectral features. Different secondary structures are indicated as follows: random coil or β turns, coil; β structure, zig-zag; α -helix, gray rectangle.

suggesting that in the first case, an artifactual folding occurs. Also, the fact that the secondary structure composition observed in solution for the mixture BinA/BinB, and also for the individual proteins, is so different from the membrane associated species, suggests that a successful crystallization of the binary toxin in either case would not shed light on its functional mechanism.

Acknowledgments

This work was supported by the Thailand Research Fund (to P.B.) and the Biomedical Research Council (BMRC) of Singapore (to J.T.).

References

- J.F. Charles, C. Nielson-LeRoux, A. Delecluse, *Bacillus sphaericus* toxins: molecular biology and mode of action, Annu. Rev. Entomol. 41 (1996) 451–472.
- [2] P. Baumann, M.A. Clark, L. Baumann, A.H. Broadwell, *Bacillus sphaericus* as a mosquito pathogen: properties of the organism and its toxins, Microbiol. Rev. 55 (1991) 425–436.
- [3] A.G. Porter, E.W. Davidson, J.W. Liu, Mosquitocidal toxins of bacilli and their genetic manipulation for effective biological control of mosquitoes, Microbiol. Rev. 57 (1993) 838–861.
- [4] E.W. Davidson, C. Oei, M. Meyer, A.L. Bieber, J. Hindley, C. Berry, Interaction of the *Bacillus sphaericus* mosquito larvicidal proteins, Can. J. Microbiol. 36 (1990) 870–878.
- [5] L. Nicolas, A. Lecroisey, J.F. Charles, Role of the gut proteinases from mosquito larvae in the mechanism of action and the specificity of the *Bacillus sphaericus* toxin, Can. J. Microbiol. 36 (1990) 804–807.
- [6] A.H. Broadwell, P. Baumann, Proteolysis in the gut of mosquito larvae results in further activation of the *Bacillus sphaericus* toxin, Appl. Environ. Microbiol. 53 (1987) 1333–1337.
- [7] C. Oei, J. Hindley, C. Berry, Binding of purified *Bacillus sphaericus* binary toxin and its deletion derivatives to *Culex quinquefasciatus* gut: elucidation of functional binding domains, J. Gen. Microbiol. 138 (1992) 1515–1526.
- [8] M.H. Silva-Filha, C. Nielsen-Leroux, J.F. Charles, Identification of the receptor for *Bacillus sphaericus* crystal toxin in the brush border

- membrane of the mosquito *Culex pipiens* (Diptera: Culicidae), Insect Biochem. Mol. Biol. 29 (1999) 711–721.
- [9] I. Darboux, C. Nielsen-Leroux, J.F. Charles, D. Pauron, The receptor of *Bacillus sphaericus* binary toxin in *Culex pipiens* (Diptera: Culicidae) midgut: molecular cloning and expression, Insect Biochem. Mol. Biol. 31 (2001) 981–990.
- [10] E.W. Davidson, C. Shellabarger, M. Meyer, A.L. Bieber, Binding of the *Bacillus sphaericus* mosquito larvicidal toxin to cultured insect cells, Can. J. Microbiol. 33 (1987) 982–989.
- [11] J.F. Charles, Ultrastructural midgut events in Culicidae larvae fed with *Bacillus sphaericus* 2297 spore/crystal complex, Ann. Inst. Pasteur Microbiol. 138 (1987) 471–484.
- [12] C. Cokmus, E.W. Davidson, K. Cooper, Electrophysiological effects of *Bacillus sphaericus* binary toxin on cultured mosquito cells, J. Invertebr. Pathol. 69 (1997) 197–204.
- [13] J.L. Schwartz, L. Potvin, F. Coux, J.F. Charles, C. Berry, M.J. Humphreys, A.F. Jones, I. Bernhart, S.M. Dalla, G. Menestrina, Permeabilization of model lipid membranes by *Bacillus sphaericus* mosquitocidal binary toxin and its individual components, J. Membr. Biol. 184 (2001) 171–183.
- [14] S.A. Tatulian, Attenuated total reflection Fourier transform infrared spectroscopy: a method of choice for studying membrane proteins and lipids, Biochemistry 42 (2003) 11898–11907.
- [15] J. Torres, T.J. Stevens, M. Samso, Membrane proteins: the 'Wild West' of structural biology, Trends Biochem. Sci. 28 (2003) 137–144.
- [16] B. Promdonkoy, P. Promdonkoy, M. Audtho, S. Tanapongpipat, N. Chewawiwat, P. Luxananil, S. Panyim, Efficient expression of the mosquito larvicidal binary toxin gene from *Bacillus sphaericus* in *Escherichia coli*, Curr. Microbiol. 47 (2003) 383–387.
- [17] J. Torres, P.D. Adams, I.T. Arkin, Use of a new label, (13)==(18)O, in the determination of a structural model of phospholamban in a lipid bilayer. Spatial restraints resolve the ambiguity arising from interpretations of mutagenesis data, J. Mol. Biol. 300 (2000) 677-685.
- [18] D.M. Byler, H. Susi, Examination of the secondary structure of proteins by deconvolved FTIR spectra, Biopolymers 25 (1986) 469– 487.
- [19] Y.N. Chirgadze, O.V. Fedorov, N.P. Trushina, Estimation of amino acid residue side-chain absorption in the infrared spectra of protein solutions in heavy water, Biopolymers 14 (1975) 679–694.
- [20] D. Marsh, Infrared dichroism of twisted beta-sheet barrels. The structure of *E. coli* outer membrane proteins, J. Mol. Biol. 297 (2000) 803–808
- [21] C. Ege, K.Y. Lee, Insertion of Alzheimer's A beta 40 peptide into lipid monolayers, Biophys. J. 87 (2004) 1732–1740.
- [22] E. Gazit, P. La Rocca, M.S. Sansom, Y. Shai, The structure and organization within the membrane of the helices composing the poreforming domain of *Bacillus thuringiensis* delta-endotoxin are consistent with an "umbrella-like" structure of the pore, Proc. Natl. Acad. Sci. USA 95 (1998) 12289–12294.
- [23] L.K. Tamm, S.A. Tatulian, Infrared spectroscopy of proteins and peptides in lipid bilayers, Q. Rev. Biophys. 30 (1997) 365–429.
- [24] H. Torii, M. Tasumi, Model calculations on the amide-I infrared bands of globular proteins, J. Chem. Phys. 96 (1992) 3379–3387.
- [25] A.W. Smith, A. Camara-Artigas, D.C. Brune, J.P. Allen, Implications of high-molecular-weight oligomers of the binary toxin from *Bacillus sphaericus*, J. Invertebr. Pathol. 88 (2005) 27–33.
- [26] B. Rost, C. Sander, Prediction of protein secondary structure at better than 70% accuracy, J. Mol. Biol. 232 (1993) 584–599.

Cys31, Cys47 and Cys195 in BinA are essential for toxicity of a binary toxin from

Bacillus sphaericus

Boonhiang Promdonkoy, PhD. 1,*, Patcharee Promdonkoy, BSc. 1, Busabun Chaisalee, MSc. 2,

Panadda Boonserm, PhD.² and Sakol Panyim, PhD.^{2,3}

¹BIOTEC Central Research Unit, National Center for Genetic Engineering and

Biotechnology, National Science and Technology Development Agency, 113

Phahonyothin Road, Klong 1, Klong Luang, Pathumthani 12120, Thailand

²Institute of Molecular Biology and Genetics, Mahidol University, Salaya Campus,

Nakhonpathom 73170, Thailand

³Department of Biochemistry, Faculty of Science, Mahidol University, Rama 6 Road,

Bangkok 10400, Thailand

Running title: Cysteine is required for BinA activity

Acknowledgements

This work was supported by the National Center for Genetic Engineering and

Biotechnology, National Science and Technology Development Agency, Thailand, the

Thailand Research Fund and the Commission on Higher Education, Thailand.

*Corresponding to: B. Promdonkoy, Tel: +662 564 6700 ext. 3340, Fax: +662 564 6707,

Email: boonhiang@biotec.or.th

Cys31, Cys47 and Cys195 in BinA are essential for toxicity of a binary toxin from *Bacillus sphaericus*

Abstract

The mosquito larvicidal binary toxin produced by *B. sphearicus* composes of 2 proteins called BinA and BinB. While BinB acts as specificity determinant, BinA is expected to bind to BinB, translocates into cytosol and exerts its activity via unknown mechanism. To study the role of cysteine in BinA, 3 cysteine residues were substitututed by alanine and serine. Substitution at Cys195 significantly reduced the toxin activity whereas substitution at Cys31 and Cys47 abolished its toxicity. Intrinsic fluorescent analysis suggested that all mutant proteins should have similar tertiary structure to that of the wild type. Analysis of the mutant protein on SDS-PAGE with and without reducing agent indicated that all 3 cysteine residues did not involve in disulfide bond formation within BinA molecule. This is the first report to demonstrate that cysteine residues at 3 positions in BinA are required for full toxicity of the binary toxin. They may play a critical role during oligomerization or interaction between BinA and BinB to form the active complex.

Introduction

Binary toxin produced by some strains of *Bacillus sphaericus* is specifically toxic to *Culex* and *Anopheles* mosquito larvae. The toxin consists of 2 proteins with molecular weight about 42 kDa called BinA and 51 kDa called BinB. Both proteins are produced during sporulation phase as crystalline inclusion [17]. Upon ingestion by susceptible larvae, the protein crystals are solubilized in the alkaline condition of the larval gut. The solubilized proteins are cleaved at both N- and C-termini by the gut proteases to produce the active components [6, 8, 11]. The activated BinB is expected to bind to the receptor present on the gut cell membrane [20]. The activated BinA will then bind to BinB or BinB-receptor complex, translocate into the cytosol and exert its activity via unknown mechanism [16].

Three-dimensional structure of *B. sphaericus* binary toxin is currently unavailable. In addition, its homology model generated *in silico* is not reliable since the toxin is a unique protein showing very low homology to other protein with known structure in the database. However, both components (BinA and BinB) share 25% amino acid identity and 40% similarity to each other. It is therefore expected that both proteins should have similar 3D structures. There are some reports describing crystal formation of BinB [10] and binary toxin [21] for X-ray crystallography but no 3D structure has been reported. Analyses using biophysical techniques suggested that binary toxin produced by *B. sphaericus* present as heterotetamer consisting of 2 molecules BinA and 2 molecules BinB [22]. Combining evidence from many experiments together with computer analysis, Yuan et al. [26] proposed that BinA consists of 2 domains. The N-terminal domain about 136 amino acids should interact with BinB. Amino acids playing important role for this interaction may lie between positions 93-104 [2, 26]. The C-terminal domain from position 150 onward may be responsible for toxic action. However, there is no clear evidence to show what residues are really required for the above functions.

Amino acid sequence analysis of BinA proteins from different strains of *B. sphaericus* revealed that all of them share very high homology with more than 97% amino acid identity [1, 2]. All of them contain 3 cysteine residues at positions 31, 47 and 195. To demonstrate that these residues are important for the toxicity, site-directed mutagenesis was employed to replace those residues with alanine and serine. Effects of amino acid substitutions on expression level, inclusion formation, overall conformation and toxicity to mosquito larvae were investigated.

Materials and Methods

Bacterial strains, plasmids and oligonucleotides

E. coli K-12 JM109 previously described by Yanisch-Perron et al. [25] was used as host cells for cloning of the toxin genes. E. coli BL21(DE3)pLysS (Novagen, USA) was used for expression of the binary toxin gene. The recombinant plasmids pET-42f and pET-51f carrying BinA and BinB toxin genes, respectively, were as previously described [19]. Mutagenic oligonucleotide primers were purchased from Sigma Proligo (Singapore). The forward primer sequences are C31A; 5'-GTA TCC TTT CGC TAT ACA TGC A-3', C31S; 5'-TAT CCT TTC TCG ATC CAT GCA CCC T-3', C47A; 5'-GAC AGA AAT CGC GAG CAG AGA AAT-3', C47S; 5'-GAC AGA AAT CTC GAG CAG AGA AAA T-3', C195A; 5'-ACT CTT ATC CCG GCC ATA ATG GTT TCG-3' and C195S; 5'-TCT TAT CCC ATC GAT CAT GGT TTC G-3'. Sequences of the reversed primers are complementary to the above primers.

Construction of BinA mutants

The method used in this work was based on Stratagene's QuikChange™ Site-Directed Mutagenesis Kit. The recombinant plasmid pET-42f containing the wild type BinA gene was

used as a template for this reaction together with appropriate primers. The recombinant plasmids obtained for each mutant was transformed into *E. coli* JM109. The plasmid was extracted and analyzed by restriction endonuclease digestion. DNA sequences of the full-length *BinA* gene from all mutants were verified by automated DNA sequencer at Macrogen Inc., Korea.

Protein preparation

To test the expression of the mutant genes, each recombinant plasmid was transformed into *E. coli* BL21(DE3)pLysS. The resulting transformants were grown in LB broth containing 100 μg ampicillin/ml and 34 μg chloramphenicol/ml until OD₆₀₀ reached 0.4. One mM IPTG (isopropyl-β-D-thiogalactopyranoside) was added and the culture was further grown for at least 5 hours. The final cultures were then collected and analyzed by SDS-PAGE [14]. Protein inclusions produced in *E. coli* were released from cells using ultrasonication and partially purified using differential centrifugation as described earlier [18]. Protein inclusions were solubilized in 25 mM NaOH at 25°C for 1 hour. The solubilized protein was dialyzed in large volume of 50 mM Na₂CO₃ pH 10.5 at room temperature. The dialyzed protein was further purified by gel filtration using Superdex 200, 10/300 GL column (GE healthcare) on AKTA machine. Concentration of the solubilized protein was determined by Bradford's method [5] using Bio-Rad protein assay reagent (Bio-Rad, USA) and BSA as standard.

Mosquito larvicidal assays

Mosquito larvicidal assays were performed as described previously [18]. Three independent experiments were carried out in duplicate using 2nd instar *C. quinquefasciatus* larvae supplied by the mosquito rearing facility from the Institute of Molecular Biology and Genetics, Mahidol University. Mosquito larvicidal activity was tested by mixing BinA and

BinB inclusions at 1:1 molar ratio and diluted as 2-fold serial dilution. Six to eight concentrations were used for each toxin. One ml of diluted protein was added to 1 ml of water containing 10 larvae in each well of 24-well tissue culture plate (diameter of the well is 1.5 cm). Mortality was recorded after incubation at 30°C for 48 hours. LC₅₀ was determined using Probit analysis [13].

Results and Discussion

Mutation at Cys31, Cys47 and Cys195 should not affect protein production, inclusion formation and the overall conformation of BinA

In order to access the function of Cys31, Cys47 and Cys195, 6 single-amino acid substitutions were performed (C31A, C31S, C47A, C47S, C195A and C195S). In addition, double mutations (C31A:C47A, C31A:C195A and C47A:C195A) and triple mutation (C31A:C47A:C195A) were also generated. All mutant genes were cloned and expressed in *E. coli* BL21(DE3)pLysS. Upon induction with IPTG all mutant proteins were highly produced as inclusion bodies inside the cell at comparable level to that of the wild type. The inclusions were clearly visible inside the cell under phase-contrast microscope. Since the inclusions are insoluble and have higher density than other *E. coli* proteins, they could be released from cells using ultrasonication and separated from other cytosolic proteins by repeated washing and centrifugation. The partially purified inclusions were analyzed on SDS-PAGE (Figure 1). All mutant proteins showed comparable yield to that of the wild type. These results clearly showed that replacements at Cys31, Cys47 and Cys195 by alanine or serine did not affect protein expression and inclusion formation of BinA. Furthermore, double and triple mutations at these positions did not have any effect on expression and inclusion formation of the toxin.

Since the 3D structures of BinA and BinB have not been elucidated, it is not known what interactions that three cysteine residues at these positions may have with the neighboring residues. Therefore, to determine effect of amino acid substitutions on protein structure, the intrinsic fluorescent spectra of all mutants were analyzed comparing to that of the wild type. This technique has been successfully used to investigate conformational changes of several proteins such as cytochrome C [15], lectin [23] and horseradish peroxidase [24]. This technique was applied to determine the overall conformation of the BinA mutants comparing to the wild type. It was found that all mutant proteins exhibited similar emission spectra to that of the wild type (not shown). There was no shift in emission maximum wavelength (emission peak). These results suggested that all mutant proteins should have similar conformation to the wild type. Therefore amino acid substitutions at Cys31, Cys47 and Cys195 should not have any effect to the overall conformation of BinA.

Cys31, Cys47 and Cys195 may not involve with the disulfide bond formation within BinA molecule

Disulfide bond is a covalent bond that links 2 cysteine residues. This bond plays important role for maintaining 3D structure and function of some proteins such as growth hormone [7] and Cry4Aa [3]. There are 3 cysteine residues that are conserved in all BinA proteins from different *B. sphaericus* strains. To investigate whether these residues are involved in disulfide bond formation, the wild type and mutant proteins were subjected to analyze on SDS-PAGE with and without reducing agent (10 mM DTT). Two different sample preparations were used in this analysis. The first sample preparation used partially purified inclusions and the second preparation used proteins that were solubilized in 25 mM NaOH and subsequently dialyzed in 50 mM Na₂CO₃ pH 10.5. Samples from both preparations were mixed with SDS-PAGE sample buffer with and without 10 mM DTT and

boiled for 10 min before analyzed by SDS-PAGE. Results in figure 2 demonstrated that the mobility of the major band corresponding to BinA protein was not different between samples with and without reducing agent. These results indicated that neither intra- nor intermolecular disulfide bond was formed within BinA or between the neighboring BinA molecules.

Analysis of binary toxin extracted from *B. sphaericus* using SDS-PAGE, MALDI-TOF mass spectrometry and Dynamic light scattering demonstrated that the toxin existed as oligomer containing 2 molecules of BinA and 2 molecules of BinB [22]. This oligomer may not hold together by intermolecular disulfide bond since the oligomer band could be observed on SDS-PAGE whether or not the reducing agent was added. However, in absent of reducing agent most of the binary toxin formed very large aggregate and did not enter the gel [22]. This aggregate was not observed in our experiment because BinA protein was separately expressed and purified (Figure 2). These results indicated that intermolecular disulfide bond between BinA and BinB play important role for oligomerization of the binary toxin. There are 6 cysteine residues in BinB but only 3 of them are in the active region (Cys67, Cys161 and Cys241) and the other 3 residues were removed after proteolytic processing [11]. It is possible that one or more cysteine residues in BinA could participate in disulfide bond formation with Cys67, Cys161 and Cys241 in BinB.

Cys31, Cys47 and Cys195 are required for toxicity of BinA

Mosquito-larvicidal assay revealed that alanine substitution at Cys31 and Cys47 caused a total loss of toxicity while substitution at Cys195 significantly reduced the toxicity (Table 2). It is possible that replacement with alanine, which is a small hydrophobic amino acid, would affect hydrophobicity or polarity of these regions. To further investigate the role of these positions, serine substitution was performed. Serine is very similar to cysteine in

term of molecular size and hydrophobicity but it lacks property to form disulfide bridge. The mutants C31S and C47S showed no toxicity against mosquito larvae whereas C195S mutant exhibited comparable toxicity to that of the C195A mutant. All double and triple mutants were completely inactive. These results demonstrated that Cys31 and Cys47 are critical for activity of the binary toxin whereas Cys195 is less important. Since replacement of these positions with serine could not be able to maintain the full activity of the toxn indicated that cysteine residues are required at these positions and could not be replaced by any other amino acid. The –SH group could therefore play important role for toxicity possibly via intermolecular interaction between BinA and BinB or BinB-receptor complex. Amino acid substitution in BinA should not affect receptor binding of the binary toxin because only BinB that responsible for specific binding to receptor on the gut cell membrane [9, 16] whereas BinA is required for toxicity [12, 26].

In summary, replacements of Cys31, Cys47 and Cys195 in BinA by alanine or serine did not affect protein production but significantly reduced its toxicity. These cysteine residues may not involve with disulfide bond formation within BinA molecule but could play a critical role for intermolecular interaction between BinA and BinB. We have previously reported that BinA and BinB could interact to each other leading to conformational changes [4]. These residues might be required during conformational changes to form an active complex either in solution or on the membrane and the disulfide bridge may be formed in this step. Substitutions at Cys31 and Cys47 showed much more advert effect than at Cys195 suggesting that cysteine residues at both positions play a critical role in this interaction and could not be replaced by any other amino acid.

References

- Baumann L, Broadwell AH, Baumann P (1988) Sequence analysis of the mosquitocidal toxin genes encoding 51.4- and 41.9-kilodalton proteins from *Bacillus sphaericus*. J Bacteriol 170: 2045-2050
- 2. Berry C, Hindley J, Ehrhardt AF, et al. (1993) Genetic determinants of host ranges of *Bacillus sphaericus* mosquito larvicidal toxins. J Bacteriol 175: 510-518
- 3. Boonserm P, Mo M, Angsuthanasombat C, Lescar J (2006a) Structure of the functional form of the mosquito larvicidal Cry4Aa toxin from *Bacillus thuringiensis* at a 2.8-angstrom resolution. J Bacteriol 188: 3391-3401
- Boonserm P, Moonsom S, Boonchoy C, et al. (2006b) Association of the components of the binary toxin from *Bacillus sphaericus* in solution and with model lipid bilayers.
 Biochem Biophys Res Commun 342: 1273-1278
- 5. Bradford MM (1976) A rapid and sensitive method for the quantitation of microgram quantities of protein utilizing the principle of protein-dye binding. Anal Biochem 72: 248-254
- 6. Broadwell AH, Clark MA, Baumann L, Baumann P (1990) Construction by site-directed mutagenesis of a 39-kilodalton mosquitocidal protein similar to the larva-processed toxin of *Bacillus sphaericus* 2362. J Bacteriol 172: 4032-4036
- 7. Chantalat L, Jones ND, Korber F, et al. (1995) The crystal-structure of wild-type growth hormone at 2.5 Å resolution. Protein Pept Lett 2: 333-340
- 8. Charles J-F, Nielsen-LeRoux C, Delecluse A (1996) *Bacillus sphaericus* toxins: molecular biology and mode of action. Annu Rev Entomol 41: 451-472
- 9. Charles J-F, Silva-Filha MH, Nielsen-LeRoux C, et al. (1997) Binding of the 51- and 42kDa individual components from the *Bacillus sphaericus* crystal toxin to mosquito larval

- midgut membranes from *Culex* and *Anopheles* sp. (Diptera: Culicidae). FEMS Microbiol Lett 156: 153-159
- 10. Chiou CK, Davidson EW, Thanabalu T, et al. (1999) Crystallization and preliminary X-ray diffraction studies of the 51 kDa protein of the mosquito-larvicidal binary toxin from *Bacillus sphaericus*. Acta Cryst D 55: 1083-1085
- 11. Clark MA, Baumann P (1990) Deletion analysis of the 51-kilodalton protein of the *Bacillus sphaericus* 2362 binary mosquitocidal toxin: construction of derivatives equivalent to the larva-processed toxin. J Bacteriol 172: 6759-6763
- 12. Elangovan G, Shanmugavelu M, Rajamohan F, et al. (2000) Identification of the functional site in the mosquito larvicadal binary toxin of *Bacillus sphaericus* 1593M by site-directed mutagenesis. Biochem Biophys Res Commun 276: 1048-1055
- 13. Finney D (1971) Probit analysis. 3rd edn. London, Cambridge University Press,
- 14. Laemmli UK, Favre M (1973) Maturation of the head of bacteriophage T4. I. DNA packaging events. J Mol Biol 80: 575-599
- 15. Latypov RF, Cheng H, Roder NA, et al. (2006) Structural characterization of an equilibrium unfolding intermediate in cytochrome c. J Mol Biol 357: 1009-1025
- 16. Oei C, Hindley J, Berry C (1992) Binding of purified *Bacillus sphaericus* binary toxin and its deletion derivatives to *Culex quinquefasciatus* gut: elucidation of functional binding domains. J Gen Microbiol 138: 1515-1526
- 17. Porter AG (1996) Mosquitocidal toxin, genes and bacteria: the hit squad. Parasitol Today
 12: 175-179
- 18. Promdonkoy B, Chewawiwat N, Tanapongpipat S, et al. (2003a) Cloning and characterization of a cytolytic and mosquito larvicidal δ-endotoxin from *Bacillus thuringiensis* subsp. *darmstadiensis*. Curr Microbiol 46: 94-98

- 19. Promdonkoy B, Promdonkoy P, Audtho M, et al. (2003b) Efficient expression of the mosquito larvicidal binary toxin gene from *Bacillus sphaericus* in *Escherichia coli*. Curr Microbiol 47: 383-387
- 20. Silva-Filha MH, Nielsen-LeRoux C, Charles J-F (1999) Identification of the receptor for *Bacillus sphaericus* crystal toxin in the brush border membrane of the mosquito *Culex pipiens* (Diptera: Culicidae). Insect Biochem Mol Biol 29: 711-721
- 21. Smith AW, Camara-Artigas A, Allen JP (2004) Crystallization of the mosquito-larvicidal binary toxin produced by *Bacillus sphaericus*, Acta Cryst D 60: 952-953
- 22. Smith AW, Camara-Artigas A, Brune DC, Allen JP (2005) Implications of high-molecular-weight oligomers of the binary toxin from *Bacillus sphaericus*. J Invertebr Pathol 88: 27-33
- 23. Sultan NA, Rao RN, Nadimpalli SK, Swamy MJ (2006) Tryptophan environment, secondary structure and thermal unfolding of the galactose-specific seed lectin from *Dolichos lablab*: fluorescence and circular dichroism spectroscopic studies. Biochim Biophys Acta 1760: 1001-1008
- 24. Tayefi-Nasrabadi H, Keyhani E, Keyhani J (2006) Conformational changes and activity alterations induced by nickel ion in horseradish peroxidase. Biochimie 88: 1183-1197
- 25. Yanisch-Perron C, Vieira J, Messing J (1985) Improved M13 phage cloning vectors and host strains: nucleotide sequences of the M13MP18 and pUC19 vectors. Gene 33: 103-119
- 26. Yuan Z, Rang C, Maroun RC, et al. (2001) Identification and molecular structural prediction analysis of a toxicity determinant in the *Bacillus sphaericus* crystal larvicidal toxin. Eur J Biochem 268: 2751-2760

Table 1. Mosquito larvicidal activity of the wild type and mutant proteins against *C. quinquefasciatus* larvae

BinA and BinB inclusions were mixed at 1:1 molar ratio before feeding to mosquito larvae. Mortality was recorded after feeding the toxins for 48 hours. LC₅₀ was calculated using Probit analysis from 3 independent assays. The fidulcial limit at 95% confident is shown in the parenthesis. Samples with no mortality after feeding to the larvae at high concentration (10,000 ng/ml) are regarded as inactive.

BinB +	LC ₅₀ (ng/ml)
BinA (wild type)	116 (66–164)
BinA-C31A	inactive
BinA-C31S	inactive
BinA-C47A	inactive
BinA-C47S	inactive
BinA-C195A	840 (553–1,424)
BinA-C195S	637 (488–821)
BinA-C31A:C47A	inactive
BinA-C31A:C195A	inactive
BinA-C47A:C195A	inactive
BinA-C31A:C47A:C195A	inactive

Figure legends

Figure 1. Inclusion extraction of BinA wild type and its mutants from E. coli

Inclusion bodies were released from *E. coli* cells using ultrasonication and partially purify by repeated washing and centrifugation. W, I and S represent lanes loaded with the whole cell lysate, partially purified inclusions and soluble fraction of cell lysate after sonication and centrifugation, respectively. M and WT mean protein standard markers and the wild type. Inclusions from all mutants were similar to the wild type and some of them were not shown.

Figure 2. SDS-PAGE of BinA and its mutants in present and absent of reducing agent

Inclusion bodies (A) and solubilized proteins (B) were mixed with SDS-PAGE sample buffer with or without reducing agent (+DTT or –DTT). The mixtures were boiled for 10 minutes before loaded in each lane. The mutant proteins C31S and C47S showed similar pattern to C31A and C47A whereas C195S, all double and triple mutants showed similar pattern to C195A.

Figure 1

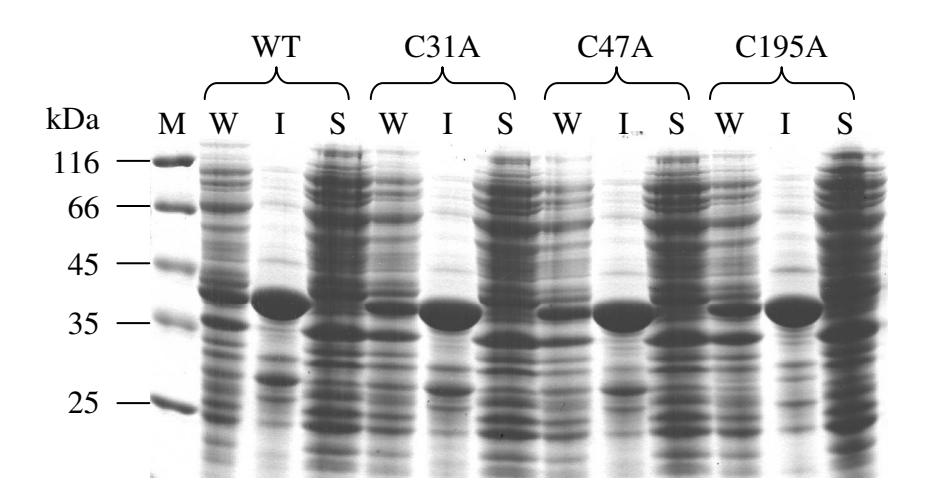
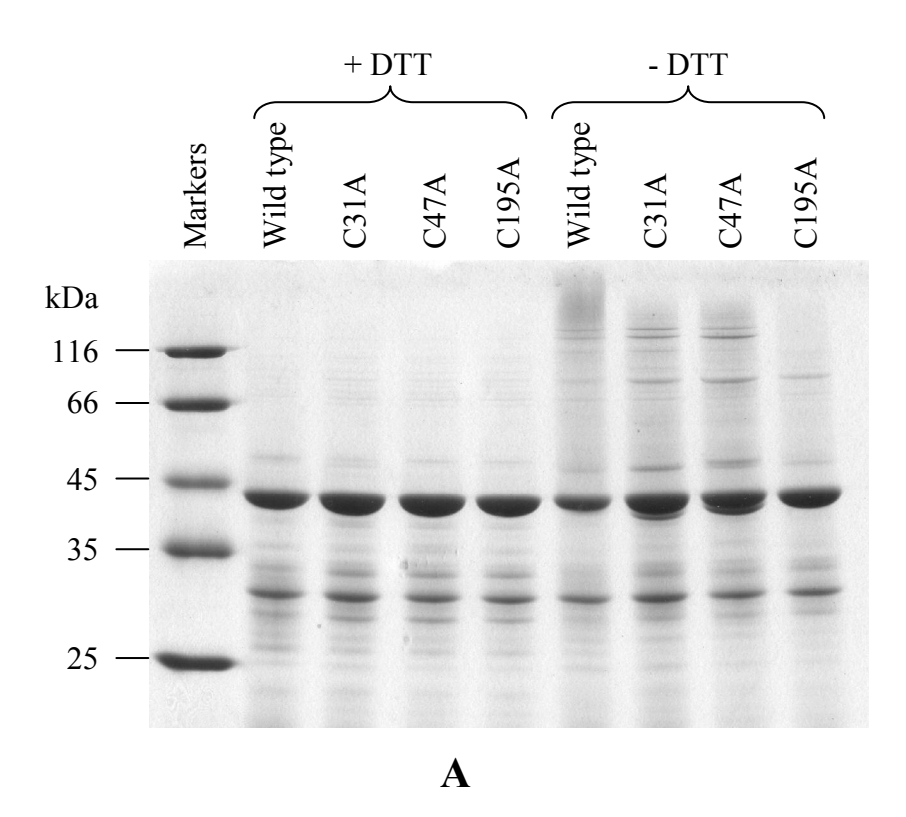
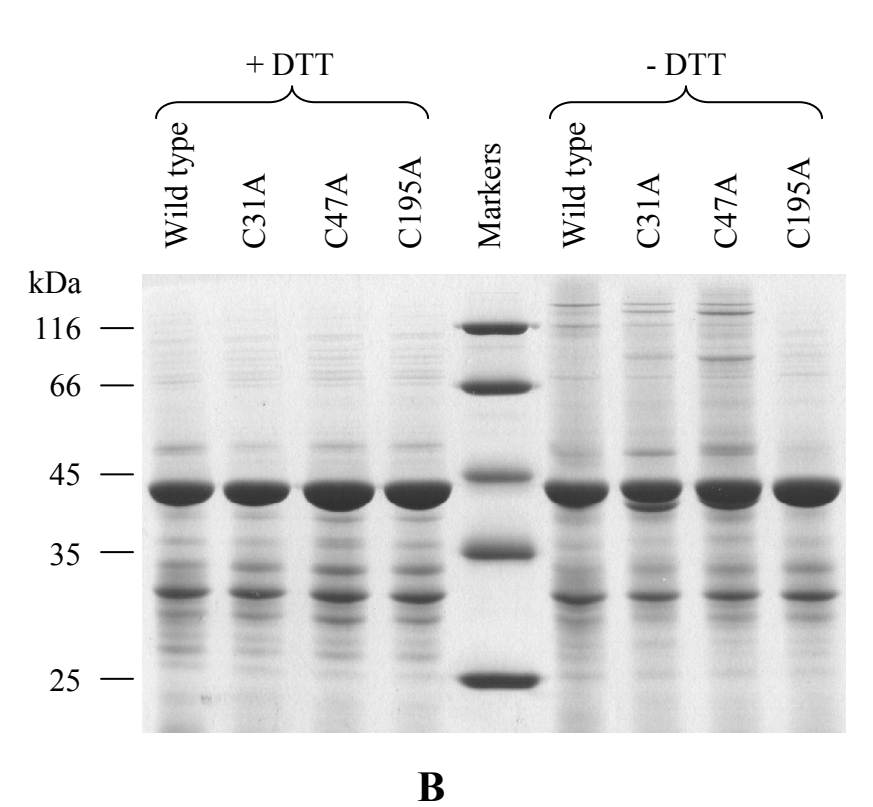


Figure 2





Springer 233 Spring Street New York, NY 10013